# Visual Function and Brain Organization in Non-decussating Retinal–Fugal Fibre Syndrome

Jonathan D. Victor[1], Patricia Apkarian[2], Joy Hirsch[1,3], Mary M. Conte[1], Maurine Packard[1], Norman R. Relkin[1], Karl H.S. Kim[1,3] and Robert M. Shapley[4]

[1]Department of Neurology and Neuroscience, The New York Presbyterian Hospital, New York, NY 10021, USA, [2]Department of Physiology, Medical Faculty, Erasmus University Rotterdam, 3000 DR Rotterdam, The Netherlands, [3]Department of Neurology, Memorial Sloan–Kettering Cancer Center, New York, NY 10021 and [4]Center for Neural Science, New York University, New York, NY 10003, USA

**Functional neuroimaging, psychophysical and electrophysiological investigations were performed in a patient with non-decussating retinal–fugal fibre syndrome, an inborn achiasmatic state in which the retinal projections of each eye map entirely to the ipsilateral primary visual cortex. Functional magnetic resonance imaging (fMRI) studies showed that for monocularly presented simple visual stimuli, only the ipsilateral striate cortex was activated. Within each hemisphere's striate cortex, the representation of the two hemifields overlapped extensively. Despite this gross miswiring, visual functions that require precise geometrical information (such as vernier acuity) were normal, and there was no evidence for the confounding of visual information between the overlapping ipsilateral and contralateral representations. Contrast sensitivity and velocity judgments were abnormal, but their dependence on the orientation and velocity of the targets suggests that this deficit was due to ocular instabilities, rather than the miswiring *per se*. There were no asymmetries in performance observed in visual search, visual naming or illusory contour perception. fMRI analysis of the latter two tasks under monocular viewing conditions indicated extensive bilateral activation of striate and prestriate areas. Thus, the remarkably normal visual behavior achieved by this patient is a result of both the plasticity of visual pathways, and efficient transfer of information between the hemispheres.**

## Introduction

Understanding the relationship of functional connections among brain areas and behavioral performance is a major goal of current neuroscience research. The visual system is a particularly useful model system to study this structure–function relationship because in the early stages of cortical visual processing information is represented as a series of retinotopic maps. We describe in detail a patient with an isolated achiasmatic state in which both temporal and nasal retinal output of each eye map to ipsilateral primary visual cortex. The overall pattern of relatively preserved visual behavior, coupled with markedly abnormal functional connectivity, provides insight into the profound plasticity of normal structure–function relationships.

The decussation of the nasal retinal fibers at the optic chiasm is essential to the normal mapping of visual information, ensuring that each hemisphere receives binocular information about the contralateral visual field. For each hemifield, the precise alignment of the retinotopic maps from each eye in the lateral geniculate nucleus (LGN) and the coincidence of the corresponding points in primary visual cortex are regarded as crucial for the organization of visual processing. Apkarian and colleagues (Apkarian *et al.*, 1994a, 1995) identified a previously undescribed congenital malformation, the absence of the optic chiasm, in two unrelated children with associated oculomotor instabilities. Misrouting of retinal fibers consistent with an absence of the optic chiasm was suggested by visual evoked potentials (VEPs), which showed activation of occipital cortex

primarily by the ipsilateral eye. The complete absence of the optic chiasm was subsequently confirmed by cranial magnetic resonance image (MRI) scans, which showed a continuous separation of the optic nerves without other associated structural defects. Monocular visual fields were full. Thus, apparently, each side of the brain receives a nearly complete, but totally monocular, map of the whole visual field. As a consequence, the anatomical organization of visual processing is fundamentally altered. This adaptive mapping is in marked contrast to the primary visual pathway organization in acquired achiasmatic deficits due, for example, to tumor (Walsh, 1956; MacCarty *et al.*, 1970) or trauma (Traquair *et al.*, 1935; Østerberg, 1938). In acquired chiasmatic anomalies, the nasal fibers are lost rather than misrouted to the ipsilateral hemisphere, resulting in bitemporal hemianopsia rather than dual complete representations.

The identification (Williams *et al.*, 1994) of a strain of mutant achiasmatic Belgian sheepdogs, also with a notable incidence of comparable oculomotor instabilities (Williams and Dell'Osso 1993), provided an animal model of the isolated chiasmal malformation. Electrophysiological exploration at the level of the LGN in the canine mutants demonstrated that retinal fibers terminated in anatomical layers that normally would receive input appropriate to the hemiretina, nasal or temporal. The aberrant nasal fibers from the *ipsilateral* eye formed a mirror-image map, in the LGN layers that ordinarily would receive nasal fibers from the *contralateral* eye.

The findings in the achiasmatic canines are comparable, albeit opposite to those in albino mammals, in which the fibers from the temporal retina near the vertical meridian erroneously decussate to the contralateral hemisphere (Lund, 1965; Guillery and Kaas, 1971; Gross and Hickey, 1980; Guillery *et al.*, 1984). In albinism, a genetic abnormality present across species, the LGN receives aberrant crossed input from temporal fibers which replaces a portion of the normal ipsilateral temporal projections. Again, each hemiretina maps to the appropriate layer of the LGN; however, the abnormal segment represents the mirror symmetric portion of the visual field, disrupting the normal alignment from layer to layer (Guillery, 1986, 1990).

The effects of chiasmal abnormalities at the cortical level have been explored in Siamese cats, homozygous for an allele of the albino gene (Guillery and Casagrande, 1977; Stone *et al.*, 1978; Guillery, 1996). In albino optic pathway misrouting, regardless of mammalian species, axons from each eye project to non-overlapping sites within the LGN, as in normal animals (Shatz, 1977; Cooper and Blasdel, 1980). Beyond the LGN, two patterns of anatomical organization of the geniculocortical pathways and respective cortical topography have been described. In one pattern (Hubel and Wiesel, 1971), termed 'Boston', primary visual cortex contains the normal hemifield representation as well as a portion of the ipsilateral temporal field, compressed in retinotopic order. The representation of the vertical meridian is

displaced from its usual position at the 17/18 border. In the other pattern (Kaas and Guillery, 1973), termed 'Midwestern', the cortical areas which receive aberrant input from the contralateral temporal retina are primarily silent, and the cats apparently do not respond to behavioral stimuli presented to the temporal retina (Elekessy *et al.*, 1973; Guillery and Casagrande, 1977). A recent review (Guillery, 1996), however, does not consider these patterns to represent mutually exclusive neural wiring strategies, and indeed the two distinct profiles of neural wiring may well coexist within a single animal (Cooper and Blasdel, 1980).

Regardless of the profile of adaptive neural organization, in both the albino and the achiasmat, the visual cortex must somehow incorporate expanded, albeit essentially monocular, information about the visual world. The achiasmat is the more extreme variant because of a total lack of input from the contralateral eye coincident with a full hemifield of aberrant input from the ipsilateral eye. For the achiasmat and as well as for the majority of albinos, the retinogeniculate miswiring is accompanied by oculomotor instabilities, the mechanism of which remains unclear (Collewijn *et al.*, 1985; Abel, 1989; Leigh and Zee, 1991; Williams *et al.*, 1994). The associated optic pathway misrouting and related oculomotor perturbations raise a variety of questions about subsequent visual processing at the cortical level. For example, how does the developmental programming of the visual cortex accommodate the profound retinogeniculate miswiring? How does the altered mapping and sensory input affect visual processing? Does convergence of monocular information occur, and if so, where? What are the effects of the anomalously organized visual system on the normal pattern of hemispheric lateralization and specialization? Previous attempts have been made to address some of these queries by studies of human albino visual function (Taylor, 1978; Loshin and Browning, 1983; Abadi *et al.*, 1989; Abadi and Pascal, 1991). However, these studies are limited primarily because of the inherently underdeveloped albino foveae and associated reduced visual acuities (Taylor, 1975; Jacobson *et al.*, 1984; Wilson *et al.*, 1988; Abadi and Pascal, 1991; Pérez-Carpinell *et al.*, 1992). Although visual behavioral studies in albino mammals also have been attempted (Creel and Sheridan, 1966; Elekessy *et al.*, 1973; Loop and Frey, 1981; Schall *et al.*, 1988), the latter are limited by the difficulty in assessing higher-order visual processing the absence of prominent hemispheric specialization.

The human achiasmats described by Apkarian and colleagues (Apkarian *et al.*, 1994a, 1995; Apkarian, 1996) have normal fundi and no associated endocrinological, neurological and/or anatomical abnormalities, thus providing a unique opportunity to address various issues and queries concerning structure–function relationships. In the present study, we describe a series of investigations performed on one of the achiasmatic patients. To distinguish the isolated condition of an absent optic chiasm from various congenital absence of the chiasm associated with other inborn midline anomalies, e.g. septo-optic dysplasia (Kaufman *et al.*, 1989; Roessmann, 1989), the naturally occurring, isolated inborn achiasmatic condition has been referred to as 'non-decussating retinal–fugal fibre syndrome'.

The study described herein was specifically designed to assess the effects of the human achiasmatic state and associated eye movement instabilities on visual pathway organization, visual function and visual perception. Investigations were designed to focus on several overlapping issues. (i) Does the abnormal retinocortical mapping affect aspects of visual function that might depend critically on precise geometrical information,

such as vernier acuity, texture perception and illusory contour formation, and does it lead to abnormal interactions between visual inputs in opposite hemifields? (ii) Are there abnormalities in visual functions that are likely to be sensitive to the ocular instabilities, such as contrast sensitivity or velocity discrimination? (iii) Given the ipsilateral-only projection pattern, do visual signals originating from the two eyes interact? (iv) What is the effect of the ipsilateral-only projection pattern on aspects of perceptual and cognitive function that involve hemispheric specialization or lateralization in normals, such as interactions of vision and language (as assayed by visual naming), visual search, attention (as assayed by an endogenous evoked potential, the P300) and illusory contour formation (Hirsch *et al.*, 1995)?

To aid the reader's navigation of this multidisciplinary study, we begin with a clinical profile, including the achiasmat's clinical history, anatomical imaging, neurological evaluation and ophthalmological/oculomotor evaluation. The individual investigations are then described. For each of the major studies, the methods, results and brief comments are presented separately. For the minor studies, results are summarized in the body of the text, and methodological details are deferred to the Appendix. These investigations were performed in four laboratories over a period of 5 days when the patient was 18 years of age, with appropriate informed consent from the patient and her parents in accord with institutional guidelines.

## Clinical Profile

### *Case History*

The patient, a fraternal twin (both females) was born at term by spontaneous delivery without complications following an uneventful third pregnancy. Birth weight was ~2500 g. Family members, including the twin sister, two older siblings (male and female) and the parents, tested negative for comparable ocular and/or optic pathway anomalies. Detailed pedigree analysis and a search for relatives with related symptoms also proved negative, suggesting a possible autosomal recessive genotype. The patient's direct clinical records report (i) ocular motor irregularities at 3 months of age, (ii) myopic refractive correction at 2 years, and (iii) nystagmus, head shudder, alternating esotropia and torticollis at 6 years. Also at the age of ~6 years, the patient presenting, in addition to ocular motor instabilities, with blond hair, fair skin and blue irides was tentatively diagnosed with possible albinism. At 9 years, the patient was referred for the VEP albino misrouting test, based primarily on the presenting ocular motor instabilities. The VEP misrouting test, implemented three times over a 5 year period, consistently revealed abnormal VEP cortical response topography. Rather than contralateral hemispheric VEP response dominance following monocular stimulation [a pathognomonic and highly reliable indication of albino optic pathway misrouting (Apkarian, 1991a,b)], the VEP response profile consistently showed ipsilateral response dominance. Repeated and appropriate visual pathway MRI imaging finally clarified the VEP results by documenting the isolated and complete absence of an optic chiasm structure (Apkarian *et al.*, 1994a, 1995; Apkarian, 1996). CT scans and MRI imaging also documented as normal other midline, subcortical or cortical structures. Around the period of the first VEP test, visual acuity was reported as 20/100 OD (right eye) and OS (left eye); visual fields and color vision were normal. Stereoscopic vision was absent. Patient medical history also revealed normal growth and endocrine function. The patient has attended regular high school, participates and performs well in gymnastics and rides a bicycle without difficulty. She does report difficulty judging the speed of vehicles in traffic and that she performs poorly in sports activities that involve throwing, catching or hitting a fast-moving target. In the last few years there has been no noticeable change in the patient's vision, except for a slight improvement due to the use of contact lenses.

### *Anatomical Imaging*

As previously reported (Apkarian *et al.*, 1994a, 1995; Apkarian, 1996), a high-resolution MRI at age 15 demonstrated complete absence of the

optic chiasm, without associated midline abnormalities. The anatomical MRI study documented the absence of auxiliary and/or accompanying midline and visual pathway abnormalities. The latter point is of particular importance to distinguish this patient's condition from other forms of chiasmal agenesis that are associated with other morphological perturbations (Maitland *et al.*, 1982; Kaufman *et al.*, 1989; Roessmann, 1989; Dutton, 1994; Menezes *et al.*, 1996). Previous CT scans showed only a broad and hypodense cisterna chiasmatis and an increased dorsum sellae to pons distance but were non-diagnostic, as were lower-resolution MRI's (Apkarian *et al.*, 1994a, 1995). High-resolution anatomical imaging, including axial and coronal scans, was pursued because of the repeated, consistent VEP evidence of optic pathway misrouting (Apkarian, 1991b).

### Neurological Evaluation

The examination was carried out in the patient's native Dutch, with the aid of a translator. The patient was alert, oriented, cooperative and right-handed. No disorders of language were noted. There was an intermittent head tilt (torticollis) to the right, with a rapid titubation. There were no dysmorphic features, and no asymmetries in sizes of digits. Detailed evaluation of cranial nerves I, V and VII–XII were entirely normal. Visual fields were full to finger confrontation with single and double simultaneous stimulation. Pupils were 5–6 mm, briskly reactive to light from nasal or temporal fields, and with consensual response to light from either field. There was a prominent nystagmus in horizontal, vertical and torsional planes. The oculomotor instabilities exacerbated in upgaze, and dampened with extreme lateral gaze, especially to the left [more detailed description and analysis of visual and oculomotor function may be found below and elsewhere (Apkarian *et al.*, 1994a,b, 1995, 1997, 1999; Apkarian, 1996)].

General motor evaluation revealed that fine finger movements (drawing circles with index finger) were slightly clumsy on the left. On first and second trials of tapping with the left foot, there was overflow to the right, but there was no overflow on repeated trials or overflow to the left with right foot tapping. The remainder of her neurological examination, including gross motor, sensory, coordination and gait testing, was normal. Additionally, simultaneous tactile stimuli presented to any two limbs were readily identified. A posture or movement passively imposed by the examiner on either hand was readily mimicked by movements of the other hand.

The patient's score on the Edinburgh Handedness Inventory (Oldfield, 1971) was +100, the maximal right-handed score.

### Ophthalmologic/Oculomotor Evaluation

Fundus examination revealed normal foveal and macular reflexes. Fundus pigmentation was light but normal. Optic disks, slightly myopic, were otherwise normal. Retinal vasculature also was normal; optic media were clear. The patient's blue irides were not diaphanous. Optical refraction resulted in spherical and cylindrical corrections with OD: S = –5.25, C = –1.5 axis 50° and OS: S = –6.75. Visual acuity was dependent upon viewing conditions. Corrected Snellen acuity at 6 m was 20/60 OD viewing, 20/100 OS viewing and 20/60 OU (both eyes) viewing. At 3 m, with OU viewing, acuity improved to –20/50, and at 20 cm (reading distance) OU acuity could reach 20/20. Interocular alignment showed an alternating esotropia of 20–25 prism diopters with preference for right eye fixation and a highly variable hypotropia (2–5°) of the left eye also during right eye fixation. Color vision tested with Ishihara plates was normal. Stereopsis tested with Titmus plates, TNO and Julesz stereograms was absent.

As reported previously (Apkarian *et al.*, 1995; Apkarian, 1996), static perimetry revealed normal visual fields; normal kinetic perimetry was confirmed during the present study. For kinetic perimetry testing, minor field instabilities at primary position were recorded due to the patient's oculomotor instabilities. However, for both static and kinetic perimetry,

the blind spot was accurately plotted and the measured vertical, horizontal and oblique meridians demonstrated 100% function.

Multiplanar eye movements recorded (Apkarian, 1996; Apkarian *et al.*, 1997, 1999) with highly accurate two- and three-dimensional scleral induction coil methods (Robinson, 1963; Ferman *et al.*, 1987) revealed eye movement instabilities in the horizontal planes characteristic of classic congenital nystagmus (Yee *et al.*, 1976; Daroff *et al.*, 1978; Abadi and Dickinson, 1986), including well-defined foveation periods and typical congenital nystagmus waveforms. Oculomotor instabilities in the vertical and torsional planes also were present and followed profiles characteristic of classic see-saw nystagmus (Maddox, 1914), with intorsion and upward movement of one eye and simultaneous extorsion and downward movement of the fellow eye (Apkarian *et al.* 1999). Velocities depended strongly on viewing distance, target position and patient attention.

## Functional Imaging Studies

### Motivation

The initial fMRI investigations were designed to confirm the ipsilateral occipital projection of the visual pathways and to establish whether there were corresponding anomalies in sensorimotor pathways. Subsequent fMRI investigations examined the pattern of activation in object naming and illusory contour perception. These more complex visual tasks were of particular interest because of the known hemispheric asymmetries such as left-hemisphere dominance for language, and (Hirsch *et al.*, 1995) a tendency for right-hemisphere dominance for illusory contour completion.

### Methods

#### Stimulation

Full-field flash visual stimulation was accomplished via red LED goggles (Grass Instruments Model S10VSB) set to flash at 8 Hz. Patterned visual stimulation was provided by back-projection onto a screen located ~205 cm from the subject's visual path in front of the scanner. The patient viewed the stimuli by looking up into a slanted mirror located above the head. She was instructed to fixate a continuously visible crosshair (0.8° × 0.8°) to help maintain a stable head and eye position. Full-field high-contrast checkerboard stimuli had a check size of 1° and a field size of 12° × 12°, and were contrast-reversed at 8 Hz. Hemifield checkerboards consisted of the left-most or right-most 5 × 12 subarray of checks, and foveal checkerboards consisted of the central 4 × 4 subarray of checks. Illusory contour stimuli consisted of Kanizsa squares (see Fig. 5) and related configurations that subtended ~4.5°, with the corner elements (inducers) subtending 2°. For language tasks, visual stimuli consisted of black-and-white line-drawings of objects taken from the Boston Naming Test (Kaplan *et al.*, 1983), presented to occupy approximately an 8° × 8° field centered around fixation. Visual stimulation was either monocular or binocular, as specified below; the non-viewing eye was covered by an opaque occluder.

Sensorimotor activation consisted of self-paced finger–thumb tapping, with each hand tested separately.

#### Imaging

Images were acquired on a 1.5 T GE scanner equipped for echoplanar imaging. A standard quadrature head coil (GE) was employed for initial studies of monocular full-field reversing checkerboard stimulations, illusory contours, sensory/motor stimulation and internal speech (object recognition). A 5 in. surface coil centered on the occipital pole was employed for the other stimulation conditions to optimize sensitivity in the occipital lobe. The axial planes were set parallel to a reference line

---

**Figure 1.** fMRI activations elicited by monocular viewing of a 12° contrast-reversing checkerboard, shown schematically. Left eye stimulation (*A*) activates striate (circled) and extrastriate (black arc) areas ipsilaterally. Right eye stimulation (*B*) activates striate (circled) and extrastriate (black arc) areas ipsilaterally, as well as extrastriate areas contralaterally (green arc). Color-coded voxels indicate the statistical stringency: red, *P* ≤ 0.0005; orange, *P* ≤ 0.00025; yellow, *P* ≤ 0.0001. In this and subsequent fMRI images, the black triangular wedges indicate the division between the left and right hemispheres. Ascending slice numbers correspond to the superior direction.

# Left Eye: Reversing Checkerboard

RE

LE

Ipsilateral Striate Visual Cortex

Ipsilateral Extrastriate Visual Cortex
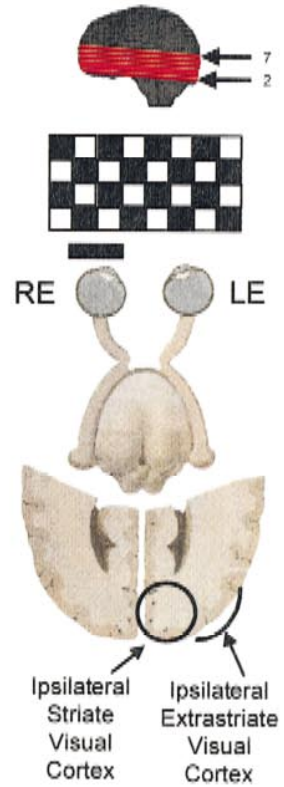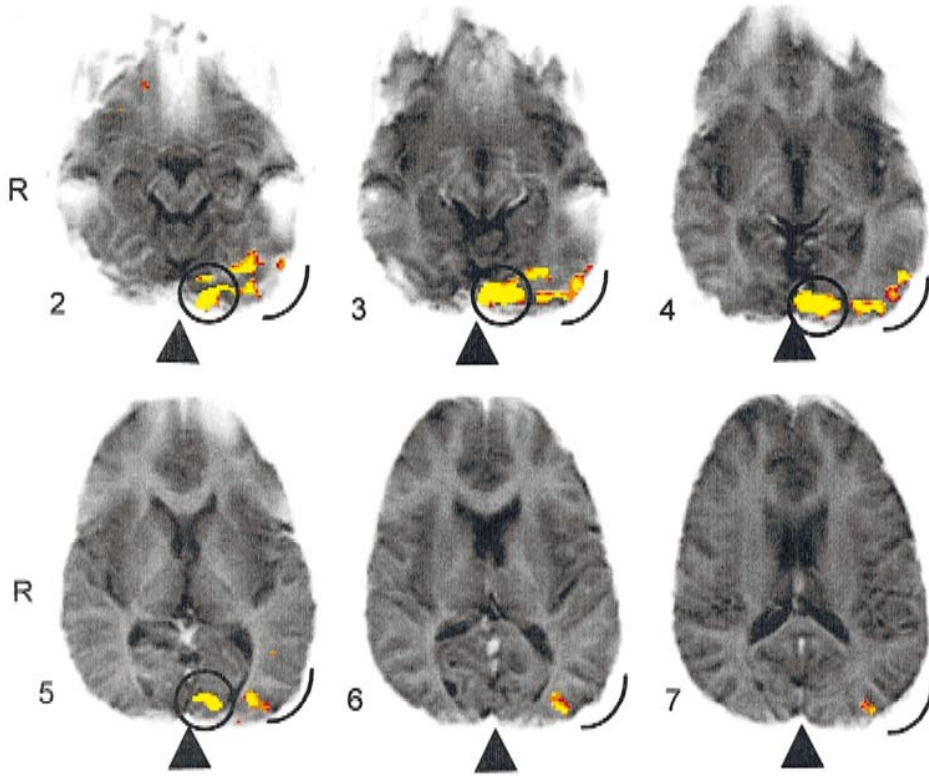
Fig 1a

# Right Eye: Reversing Checkerboard

RE

LE

Ipsilateral Extrastriate Visual Cortex

Ipsilateral Striate Visual Cortex

Contrateral Extrastriate Visual Cortex
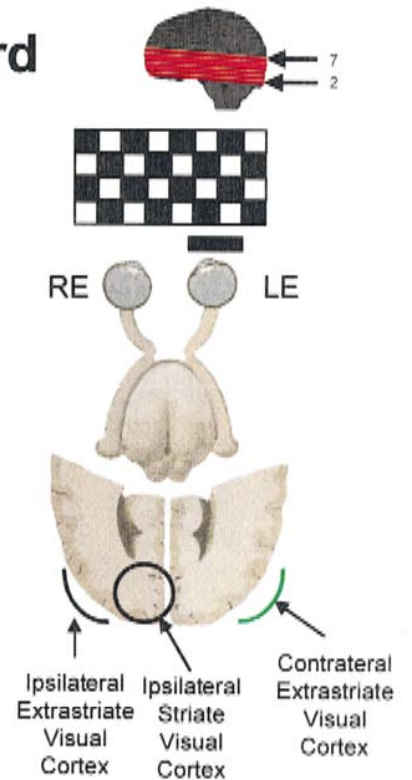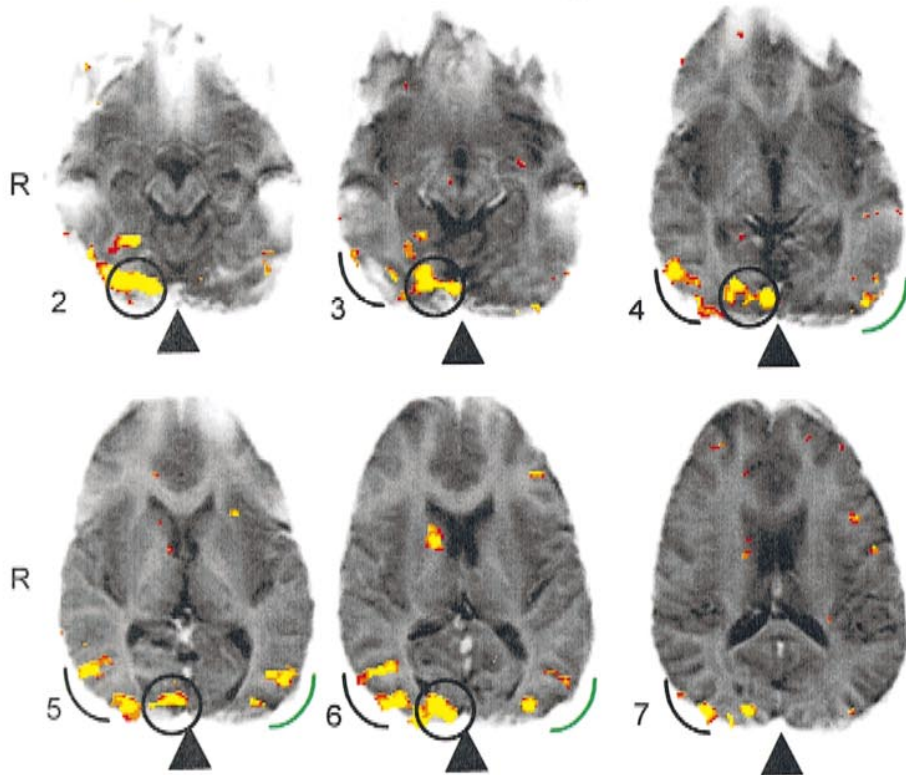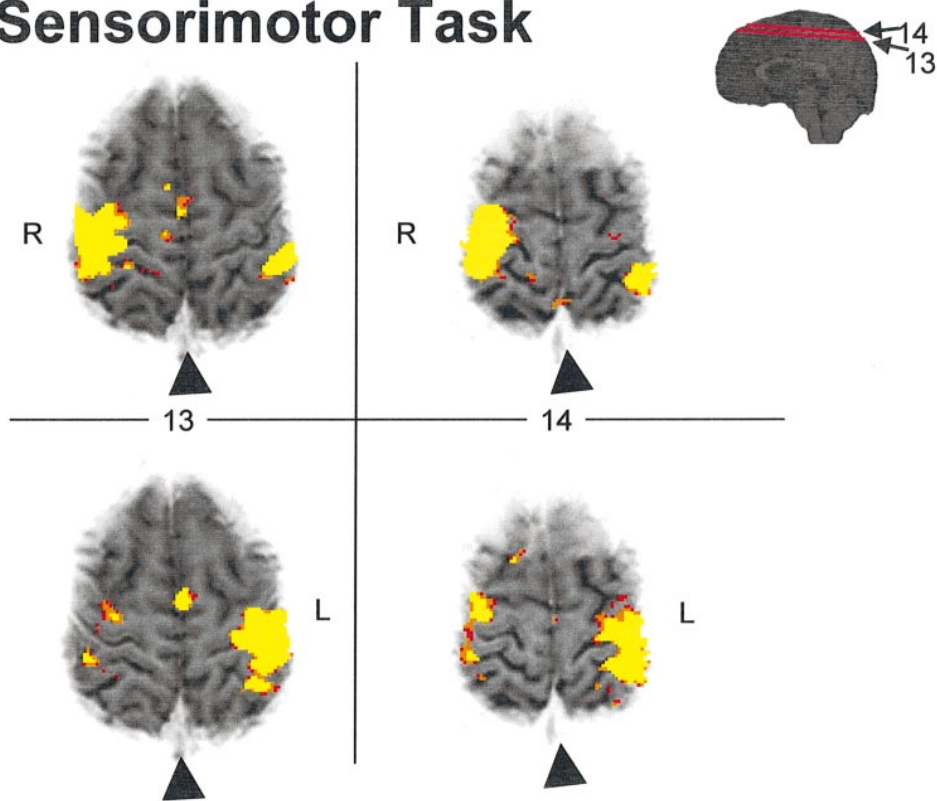
# Sensorimotor Task



**Figure 2.** fMRI activations elicited by self-paced finger–thumb tapping by the left hand (upper images) and the right hand (lower images). Sensorimotor behavior leads to predominantly contralateral activation of cortical areas surrounding the Sylvian fissure. *P*-values are color-coded as in Figure 1.

through the superior edge of the anterior commissure and the inferior edge of the inferior commissure (AC–PC line) (Talairach *et al.*, 1988) on a $T_1$-weighted midsagittal view acquired prior to each imaging session. A standard echoplanar sequence ($T_R = 3000$, $T_E = 60$, flip angle = 90°) was employed to acquire 16 contiguous slices. In the case of the global head coil studies slice thickness was 4.5 mm and covered the entire cortical area, whereas in the case of later surface coil studies slice thickness was 3.0 mm and the slices covered the occipital lobe. Otherwise all imaging methods were equivalent for both series. With these parameters, in-plane resolution was 1.6 × 1.6 mm.

Thirty images were acquired during each 90 s imaging run. The first 10 images (30 s) were acquired during a baseline period, followed by a stimulation or task period of 10 images (30 s), and a final (30 s) baseline period also consisted of 10 images. Two identical runs were performed in each condition. Prior to statistical analysis, all brain images for each session were computationally aligned for direct spatial comparisons between different tasks (Woods *et al.*, 1993), and a two-dimensional Gaussian filter (~3 volume elements, voxels, at half-height) was applied except where the highest resolution was required and then no filter was applied. Significant signal changes were identified by a multi-stage statistical analysis which compared average baseline and stimulation signal intensities and required significant signal changes on two runs (coincidence) (Hirsch *et al.*, 1995). For the criteria used in the images shown here, the fraction $p$ of false-positive voxels, empirically deter-

mined from images of a spherical phantom filled with copper sulfate solution (General Electric standard), was <0.0005, unless otherwise noted.

## Results

Figure 1 shows activations induced by 12° × 12° checkerboard stimulation of each eye. Activation in primary visual cortex was restricted to the ipsilateral hemisphere. Extrastriate activation was seen on the ipsilateral side with stimulation of either eye, and also in the contralateral hemisphere with right eye stimulation (Fig. 1*B*). In contrast, the sensorimotor task, as shown in Figure 2, elicited a crossed (i.e. predominantly contralateral) pattern of cortical activation, as expected from normal neuroanatomy (Truex and Carpenter, 1969) and consistent with findings in control subjects studied in our laboratory (J. Hirsch, M. Ruge, K.H.S. Kim, M.M. Souweidane and P. Gutin, unpublished data). Thus, we found no evidence of anomalies in sensorimotor pathways corresponding to, or induced by, the congenital miswiring of the visual pathways.

The subsequent imaging studies explored visual organization in greater detail. Figure 3*A* shows responses to both left

**Figure 3.** (*A*) fMRI activations elicited by hemifield contrast-reversing left eye stimulation. Yellow: voxels activated only during left hemiretina (right hemifield) stimulation. Red: voxels activated only during right hemiretina (left hemifield) stimulation. Orange: voxels activated in both conditions. The division between the left and right hemispheres (arrow) is tilted clockwise due to the position of the surface coil. (*B*) Statistical analysis of the number of voxels that appear to be activated, for a range of levels of stringency. Yellow: fraction of voxels activated by left hemiretina stimulation ($p_L$), including voxels activated by stimulation of both hemiretinae, derived from the number of yellow voxels *plus* the number of orange voxels in (*A*). Red: fraction of voxels activated by right hemiretina stimulation ($p_R$), including voxels activated by stimulation of both hemiretinae, derived from the number of red voxels *plus* the number of orange voxels in (*A*). Orange: fraction of voxels activated by stimulation of both hemiretinae ($p_{LR}$), derived from the number of orange voxels in (*A*). Fractions are based on a 1280 voxel region of interest, located as described in text. The fraction of voxels jointly activated by the two conditions is substantially greater than expected by chance, namely $p_L p_R$ (green).

# Left Eye: Stimulation of Left and Right Hemiretina



R

10

R

9

10
9

LE

Ipsilateral
Striate
Visual
Cortex

= Left Hemiretina
= Right Hemiretina
= Common Areas

Fig 3a



= (Left Hemiretina) Observed
= (Right Hemiretina) Observed
= (Common Voxels) Observed
= (Common Voxels) Predicted
(based on chance of overlap)
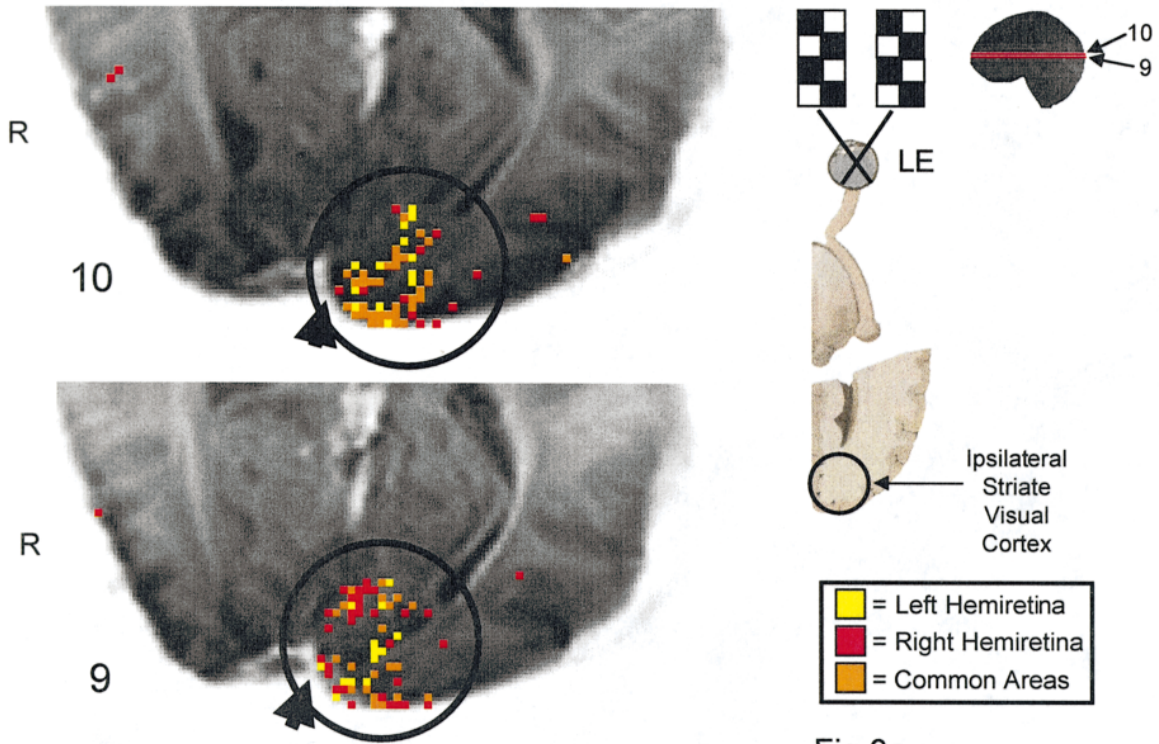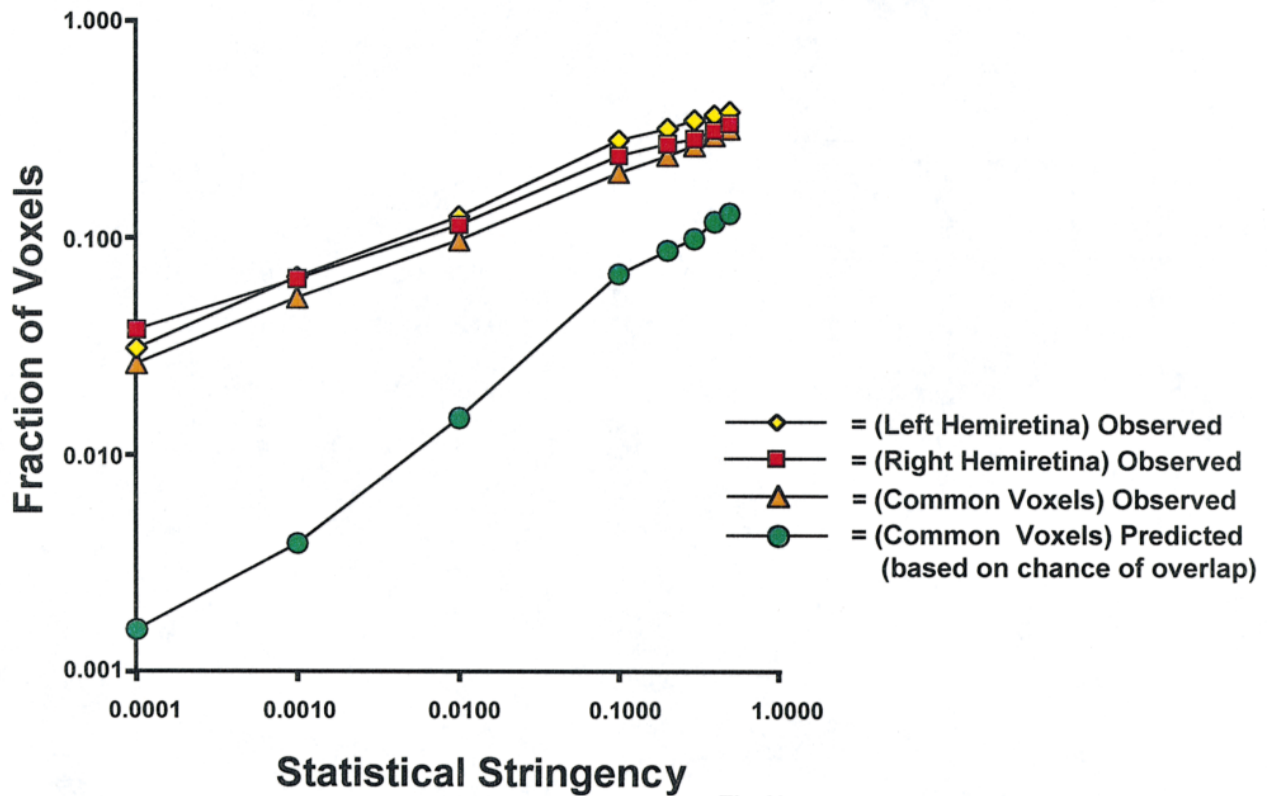
Fig 3b

hemiretina (right hemifield) and right hemiretina (left hemi-field) checkerboard stimulation OS, and illustrates the general observations for OS and OD. Voxels activated by each visual stimulation of each hemiretina occupied overlapping areas of primary visual cortex (orange), and neither hemifield detectably activated contralateral visual cortex or extrastriate areas. To determine the significance of this overlap, we performed the statistical analysis summarized in Figure 3B. The criteria in the multistage statistical analysis of each eye's image were allowed to vary, to provide a range of stringency levels (i.e. false-positive activations $p$). For each $p$-value (abscissa), the fraction of voxels activated by stimulation of left and right hemiretina ($p_L$ and $p_R$) within the occipital region of interest was determined, as was the fraction of voxels activated by both eyes ($p_{LR}$). The region of interest for this calculation consisted of a volume of 1280 voxels ($16 \times 16 \times 5$) within the brain, located by anatomical criteria alone (aligned $T_1$ images), without reference to the activation images. If joint activation were due to chance alone, then the probability of joint activation $p_{LR}$ would be approximated by the product of the probabilities of activation by either eye alone, $p_L p_R$. However, across more than a 1000-fold range of stringency levels, the number of common voxels observed was far in excess of the chance expectation. Thus we conclude that, to within the resolution of the imaging technique, stimulation of either hemifield activated overlapping regions of occipital cortex. Similar findings were present with right eye stimulation, but fewer voxels were activated.

Because the patient's oculomotor instabilities precluded a detailed analysis of the topography of the retinocortical mapping by conventional methods (Engel *et al.*, 1997), we used a customized, low-resolution strategy to demonstrate the presence of at least a rudimentary topographic map. We compared activations elicited by monocular viewing of a central $4° \times 4°$ patch of a checkerboard (presumed to stimulate primarily the fovea and parafovea) with areas activated by full-field LED flashes (presumed to stimulate the entire retina, but to be a relatively less-effective stimulus for foveal and parafoveal retinal ganglion cells sensitive to spatial contrast). As shown in Figure 4, OS viewing of the central patch activated primary visual cortex predominantly along the medial bank inferiorly (slices 3–8), while OS viewing of the full-field flash activated primary visual cortex along the medial bank more superiorly (slices 10 and 11) and also along the outer convexity (posteriorly in slices 3–6). Areas of extrastriate cortex activated by OS viewing of these stimuli were also present (anterolaterally along the outer convexity in slices 3–11). With OD viewing, the areas of striate cortex activated by the full-field flash were also spatially distinct, and followed a pattern comparable to that obtained with OS viewing. With OD viewing, striate activation extended more superiorly and extrastriate activation was relatively less prom-inent, compared to OS viewing.

Viewing of illusory-contour stimuli with OD (Fig. 5) elicited foci of activation in extrastriate areas of both hemispheres. However, the right-hemisphere foci were more extensive, and the focus of voxels activated in the left hemisphere was also activated by stimulation by the control (no illusory contour) stimulus, in which the corner elements occupied the same area of visual space but were rotated so that no illusory contour was

present. Viewing of the illusory contour stimuli OS also produced bilateral foci of activation in extrastriate cortex. As was the case for OD viewing, the left-hemisphere focus was activated by the illusory contour stimulus as well as the control, while the right-hemisphere focus was activated only by the illusory contour. For the statistical criteria we used ($P \leq 0.0005$ to $P \leq 0.0001$), the only cortical areas activated by the illusory contour stimulus but not by the control stimulus were in the right hemisphere (slice 5 for OD viewing, slice 6 for OS viewing, circled in Fig. 5). That is, with viewing either OD or OS, we identified a focus of right-hemisphere activation that was elicited by illusory contours but not by the control stimulus.

The observed patterns of activations induced by picture-naming tasks are complex, and are shown in Figure 6. With OS viewing (Fig. 6A), we observe areas of activation in ipsilateral striate (black circle) and extrastriate (black arc) cortex, and in the contralateral extrastriate (green arc) and striate (green circle) cortex. Activations were also seen more anteriorly in the left inferior frontal gyrus, putative Broca's area, and also in the corresponding portions of the right hemisphere. With OD viewing (Fig. 6B), a similar pattern of activation of both ipsilateral and contralateral striate and extrastriate cortices, as well the anterior areas described above, was seen. The activation of both Broca's area and its mirror image in this task has frequently been observed in control subjects in our lab while performing this task (Hirsch, Ruge, Kim, Souweidane and Gutin, unpublished data) and related tasks (Kim *et al.*, 1997).

### Comments

The fMRI responses to simple visual stimulation (Fig. 1) confirm the ipsilateral projection pathways of each eye to primary visual cortex, as expected from the anatomy of the patient's visual pathways and the analysis of the VEP responses (Apkarian *et al.*, 1994a, 1995). As shown by statistical analysis of the activated voxels, areas of primary visual cortex activated by left and right hemifield stimulation of the same eye were overlapping, to within the resolution ($1.6 \times 1.6$ mm in-plane) of the imaging technique (Fig. 3). Although the subject's eye movements precluded a detailed analysis of the topography of the retino-cortical map, the spatial separation of responses to central and full-field stimulation (Fig. 4) indicates that at least some topo-graphic specificity is present. Moreover, the demonstration of distinct areas of activation by a $4° \times 4°$ central checkerboard and a $12° \times 12°$ patch (Fig. 4) demonstrate that eye movements alone cannot be responsible for the nearly complete overlap of the hemifield responses (Fig. 3). Sensorimotor pathways, as assessed by our functional imaging technique, showed the normal 'crossed' organization.

Illusory contour completion is part of the visual mechanisms for segmentation of figure from ground (Petry and Meyer, 1987), but is also a crucial step for visual object recognition. Previous work (Hirsch *et al.*, 1995; Ffytche and Zeki, 1996; Mendola *et al.*, 1997) indicates that extrastriate occipital cortex in humans is activated by illusory contour stimuli, and has suggested a right-hemisphere specialization for this process (Hirsch *et al.*, 1995). The present results (Fig. 5) demonstrate in the achiasmat the presence of an extrastriate focus of activation induced by illusory contours. Moreover, cortical activation specific to the

---

**Figure 4.** fMRI activations elicited by monocular viewing of a full-field, contrast-reversing checkerboard confined to the central 4° (yellow) and full-field stimulation with flashing LED goggles (red). Voxels that were activated with both stimuli are shown in orange. Stringency level: $P \leq 0.0005$. The division between the left and right hemispheres (arrow) is tilted clockwise due to the position of the surface coil.

# Central and Full Field Stimulation



Left Eye    Right Eye    Left Eye    Right Eye

= Central 4 degrees

= Full field

= Central and Full field
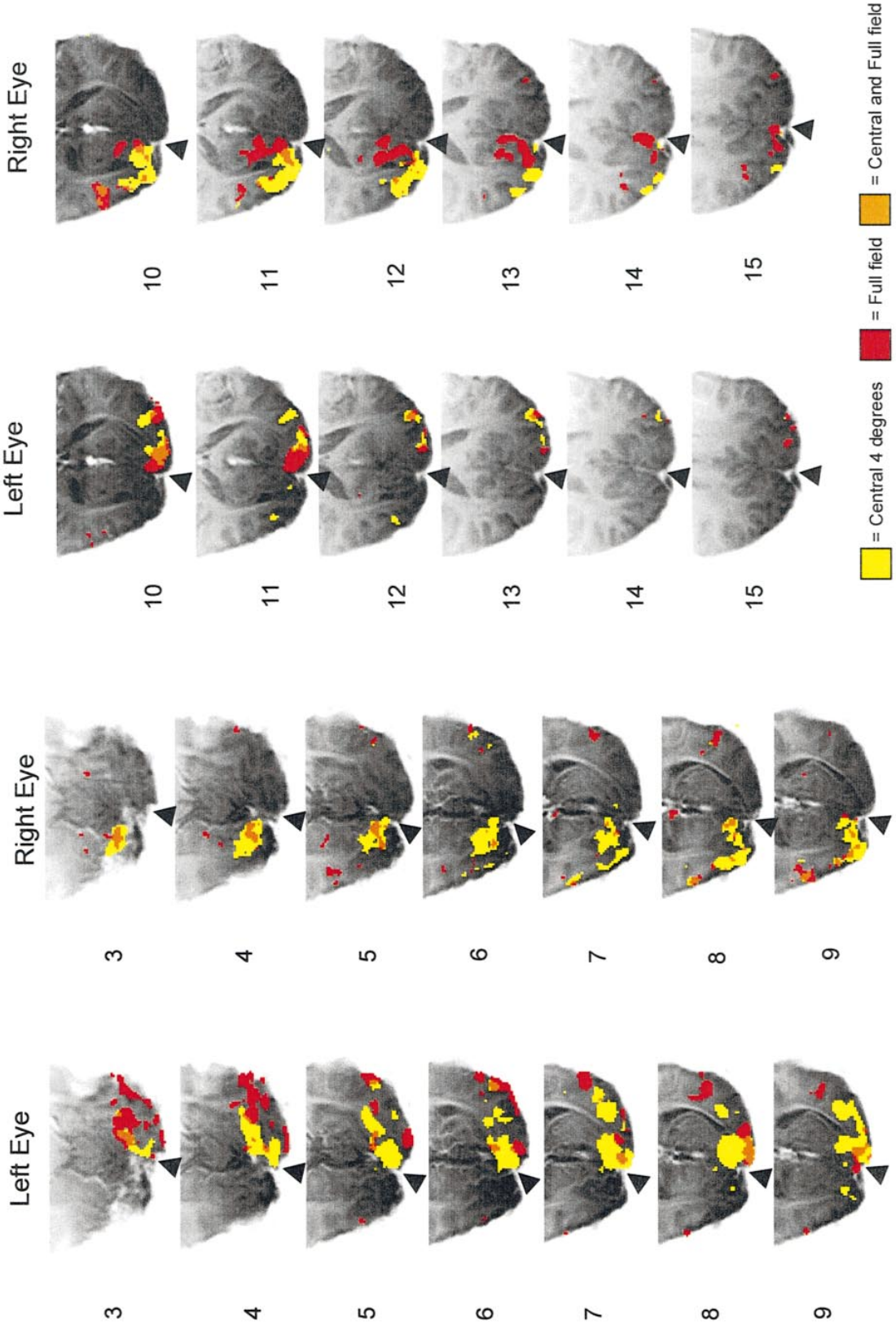
presence of the illusory contour is found predominantly in the right hemisphere, regardless of the viewing eye (and hence, regardless of side in which primary visual cortex is activated).

In some tasks, activation of contralateral visual areas was observed. This contralateral activation was progressively more prominent as the complexity of the task increased: for passive viewing of a checkerboard, the only contralateral activation observed was in extrastriate cortex, with OD viewing (Fig. 1). For illusory contour stimuli (Fig. 5), viewing with either eye elicited contralateral activation, but confined to extrastriate cortex. In the picture naming task (Fig. 6), viewing with either eye elicited contralateral activation not only of extrastriate cortex but of striate cortex as well.

## Psychophysical and Evoked Potential Studies

### Vernier Acuity

#### Motivation
As demonstrated above, each striate cortex in this patient receives projections from both ipsilateral and contralateral halves of space. Since vernier acuity requires precise geometrical information, elevated thresholds would be expected if such information were not preserved by this abnormal mapping. Furthermore, since each striate cortex represents a visual field of twice the normal extent, elevation of vernier acuity thresholds out of proportion to acuity loss might be expected from amblyopia-like 'crowding' (Levi and Klein, 1985).

#### Methods
Stimuli consisted of abutting horizontal (8 × 64 min) bars at a contrast of 0.25, presented for 1 s on a mean luminance background of 150 cd/m$^2$. Control signals for the visual stimulator (Tektronix 608) were produced by electronics modified from the design of Milkman et al. (Milkman et al., 1980). Viewing distance was 57 cm and the display size was an 8° × 8° square. In each trial, one of the two bars appeared vertically displaced. The patient was asked to indicate whether the left or the right bar was higher. A staircase algorithm (initial step size, 0.3 log units; final step size, 0.1 log units) controlled the bar displacements, and a 71% correct threshold was estimated from each staircase as the geometric mean of the final eight reversals. A final estimate of the 71% correct threshold for each viewing condition (OS, OD and OU) was taken as the geometric mean of six runs for each condition, presented in counterbalanced order.

#### Results and Comments
Displacement thresholds were: OS, 0.38 min; OD, 0.21 min; OU, 0.25 min. The difference between the thresholds for OS judgments and OD or OU judgments was not statistically significant (t-test, P > 0.05). These thresholds were in the hyperacuity range, and directly comparable to an OU threshold mean of 0.28 min obtained from six normal subjects (aged 20–38) studied under similar stimulus conditions. Thus, no abnormality in the precision of the retinocortical map or the ability of the patient to access precise geometrical information was identified.

### Completion Tasks: Illusory Contour Formation and the Street Test
Illusory contour formation, along with vernier acuity, makes use of precise geometrical information. Additionally, illusory contour formation is considered to be a critical first step in segmentation of the visual field into objects (Petry and Meyer, 1987). To study illusory contour formation, we used the Kanizsa square stimuli similar to those used in the fMRI studies, and also a more complex task, the Street test (Street, 1932) of 'Gestalt completion' (Wasserstein et al., 1987). Performance on the

Street test appears to depend in part upon the same mechanism as that studied with illusory contours, because completion of many of the incomplete contours in the Street figures involves illusory contour formation. However, the Street test also requires placing these completed contours in context as well as object recognition. On both tests (see Appendix for details), performance was normal with either eye.

### Contrast Sensitivity and Velocity Discrimination for Moving Gratings

#### Motivation
Ocular instabilities might directly affect contrast sensitivity (as a result of image blur), or velocity discrimination (as a result of retinal image motion). Additionally, the patient's sole visual complaint was of difficulty judging velocities. To determine whether these deficits were present, and to separate the effects of elevated detection thresholds on velocity discrimination, we measured detection thresholds for moving gratings and velocity discrimination thresholds at a fixed multiple of the measured detection thresholds.

#### Methods
To determine the detection threshold for drifting gratings, the patient was asked to determine which interval of two 1.25 s interval presentations contained a sinusoidal luminance grating (1 c/°, 4°/s drift velocity); in the other interval, the display remained at the mean luminance of 150 cd/m$^2$. Viewing distance was 57 cm and the display size was an 8° square. A two-alternative, forced-choice staircase algorithm (initial step size, 0.3 log units; final step size, 0.1 log units) controlled the contrast of the grating. (Contrast is defined as the Michelson contrast $[(I_{max} - I_{min})/(I_{max} + I_{min})]$.) In this study, during the monocular viewing conditions, the non-viewing eye was lightly patched with a translucent gauze.

A 71% correct contrast threshold was estimated as the geometric mean of the final eight reversal points on each staircase. For each viewing condition (OS, OD and OU), and direction of drift (upwards, downwards, leftwards and rightwards), geometric means from two staircases formed the final threshold estimate. A similar procedure was used to determine contrast thresholds for 4 c/°, 4 Hz flickering gratings.

Velocity discrimination was measured via a two-interval forced-choice method adapted from Taub et al. (Taub et al., 1997). Stimuli consisted of pairs of sequentially presented drifting gratings, each chosen from one of five velocities (2.0, 2.8, 4.0, 5.6 and 8.0°/s), and sharing the same drift direction. The patient was asked to determine which interval contained the faster grating. Grating spatial phase was randomized, and spatial frequency and presentation time were jittered by 10% to prevent the use of cues other than velocity. The contrast was set to equal 10× the threshold determined in the grating-detection experiment. A block of trials consisted of 75 such presentations for a single drift direction. On each of two days, one such block of trials was run for each viewing condition (OS, OD and OU) and each of the four drift directions. Blocks were run in an order that counterbalanced learning effects. For each condition, velocity discrimination was summarized by a Weber fraction (i.e. the fractional change in velocities necessary for 75% correct discrimination), derived from the staircase data by the method of Taub et al. (Taub et al., 1997).

#### Results
Contrast thresholds (mean of two staircase determinations) for detection of drifting 1 c/° gratings are shown in Table 1. For vertically drifting (horizontally oriented) gratings, monocular and binocular thresholds were similar, and within the range of normal subjects in our laboratory. For horizontally drifting (vertically oriented) gratings, thresholds were ~2-fold higher than for horizontally oriented gratings when viewed OD and OU, and 3-fold higher when viewed OS.

# Illusory Contour and Control

## Right Eye | Left Eye

**ILLUSORY CONTOUR** R

**CONTROL** R
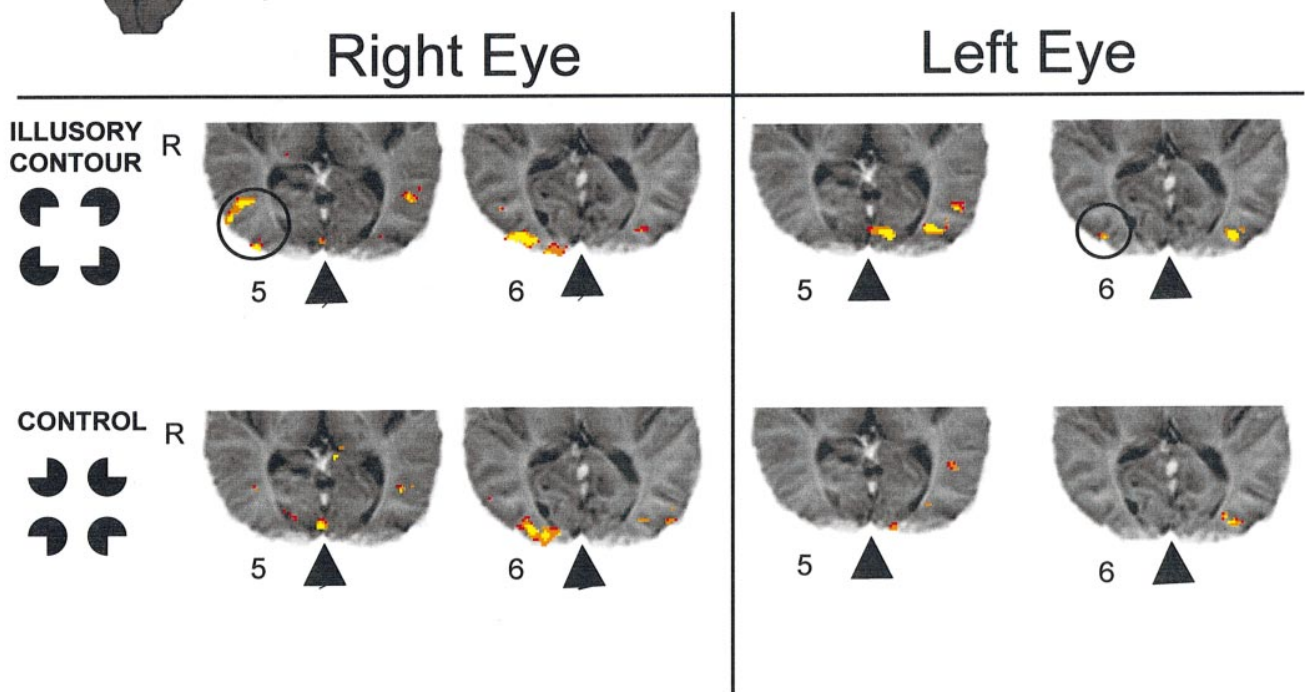
**Figure 5.** fMRI activations elicited by monocular viewing of illusory contour stimuli. The stimuli subtended 4.5°. Stringency levels are indicated by color-coding, as in Figure 1.

**Table 1**

Contrast thresholds (Michelson contrast units) for 1 c/°, 4 Hz drifting gratings and 4 c/°, 4 Hz flickering gratings

| | Vertical orientation | | | Horizontal orientation | | |
|---|---|---|---|---|---|---|
| | OS | OD | OU | OS | OD | OU |
| Drifting gratings | 0.022 | 0.012 | 0.011 | 0.006 | 0.005 | 0.005 |
| Flickering gratings | 0.017 | 0.020 | 0.022 | 0.007 | 0.008 | 0.009 |

For vertically oriented gratings, drift direction was horizontal; for horizontally oriented gratings, drift direction was vertical.

**Table 2**

Weber fractions for velocity discrimination of 1 c/° drifting gratings

| | Vertical orientation (horizontal drift) | | | Horizontal orientation (vertical drift) | | |
|---|---|---|---|---|---|---|
| | OS | OD | OU | OS | OD | OU |
| All velocities | 0.71 | 0.62 | 0.81 | 0.35 | 0.37 | 0.36 |
| Low velocities (2, 2.8, 4°/s) | [a] | 0.94 | [a] | 0.49 | 0.72 | 0.64 |
| High velocities (4, 5.7, 8°/s) | 0.41 | 0.49 | 0.38 | 0.28 | 0.20 | 0.25 |

Gratings were presented at 10× detection threshold. Estimates of the Weber fraction are made from responses to the full range of stimulus velocities (2–8°/s), as well as from responses to the lower half of the range of stimulus velocities (2–4°/s) and the upper half of the range of stimulus velocities (4–8°/s).

[a]Performance was at chance level, implying a Weber fraction of at least 1.

For velocity discrimination, there were no consistent differences between leftward and rightward drifting gratings, or between upward and downward drifting gratings, so these pairs of conditions were pooled. As summarized in Table 2, there were large and consistent differences between horizontal and vertical drifting gratings. First consider the velocity discrimination Weber fractions obtained from the full range (2–8°/s) of stimuli. For vertical drift, Weber fractions (0.35–0.37) were similar under the three viewing conditions (OS, OD, OU), but were approximately twice the velocity discrimination Weber fraction of 0.17 obtained for three normal subjects (aged 20–38) studied under similar conditions (Taub *et al.*, 1997). For horizontal drift, there was also little dependence on viewing condition, but the Weber fractions (0.62–0.81) were ~4-fold higher than the values obtained in normal subjects.

Examination of the psychometric surfaces across velocities (Fig. 7) reveals important information that is not evident from the overall Weber fractions. These contour surfaces indicate the

fraction of times that one stimulus is judged as faster, as a function of the pair of velocities being compared. The more closely spaced the contour lines, the greater precision of judgment (because a smaller ratio of velocities is required to lead to consistent judgments). Figure 7 thus indicates that velocity discrimination is poorer at low velocities than at high velocities, in that there is a greater spread of the contour lines from the main diagonal. This is most dramatic for the horizontal-drift conditions. With OD viewing, velocity comparisons of 2.0 and 2.8°/s gratings are at chance (no contour lines separating this point from the main diagonal), while velocity comparisons of 5.6 and 8.0°/s gratings are >70% correct (two contour lines' separation from the diagonal). With OS or OU viewing, velocity

**Left Eye: Picture Naming**

**Right Eye: Picture Naming**

Fig 6a

Fig 6b

# Horizontal Drift

# Vertical Drift

## OS



## OD



## OU
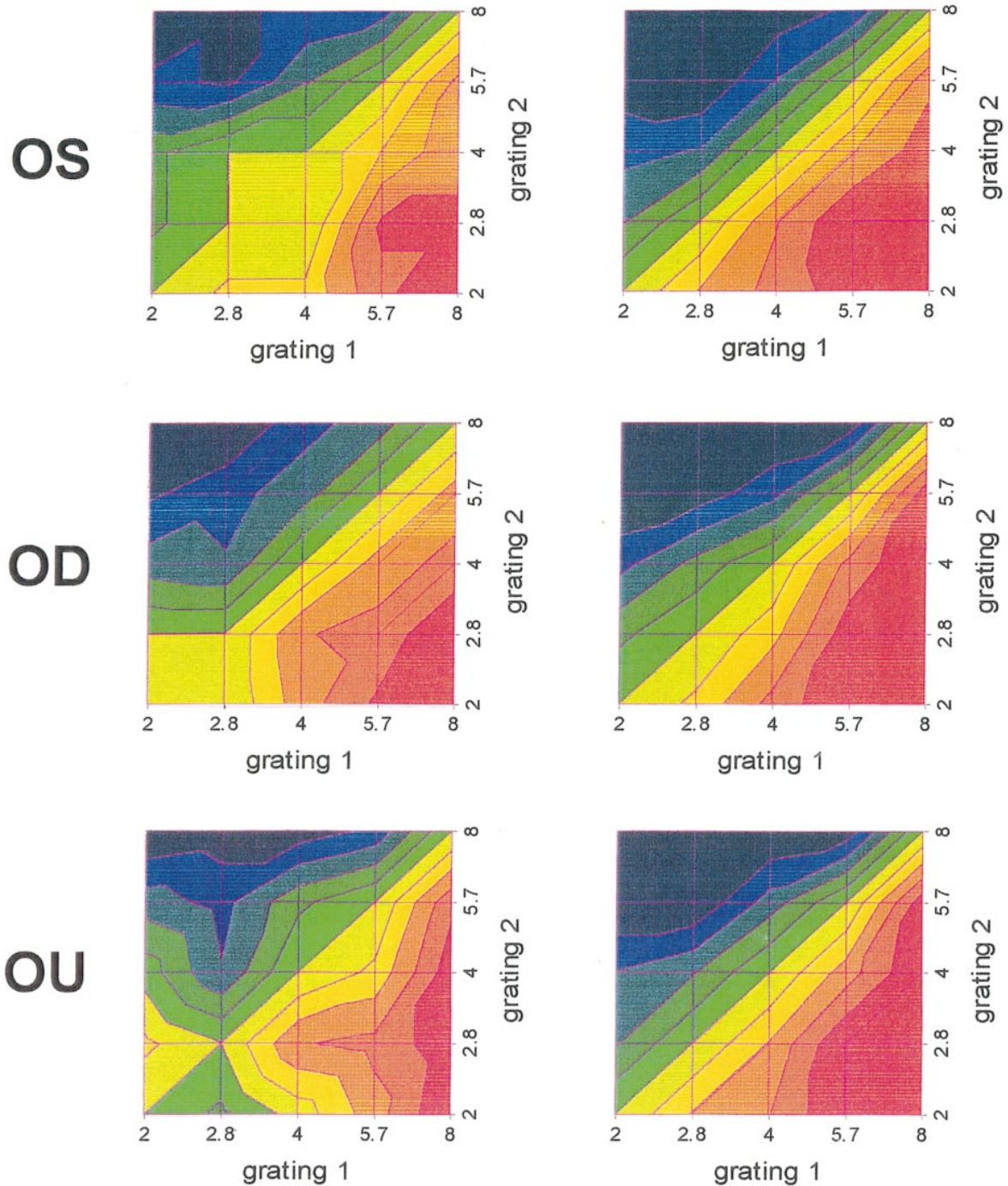


**Figure 7.** Psychometric surfaces (fraction of presentations in which the probe velocity is judged to be faster) for pairwise velocity comparisons between drifting gratings. The color-coded height of the surface at any point represents the frequency that grating 2 was judged faster than grating 1 (blue = 100%, red = 0%). Note that the surfaces are necessarily symmetric about the main diagonal, since a judgment that grating 2 is faster than grating 1 is also recorded as a judgment that grating 1 is slower than grating 2.

---

**Figure 6.** fMRI activations elicited by picture naming, with stimuli viewed monocularly: (*A*) left eye; (*B*) right eye. Stringency levels are indicated by color-coding as in Figure 1. Viewing with either eye activates striate (black, circled) and extrastriate (black arc) areas ipsilaterally, as well as activates striate (green, circled) and extrastriate (green arc) areas contralaterally.
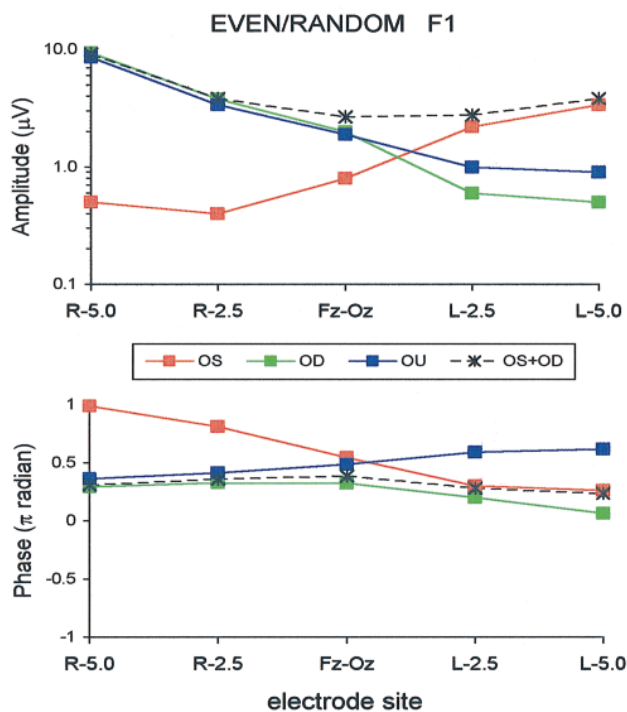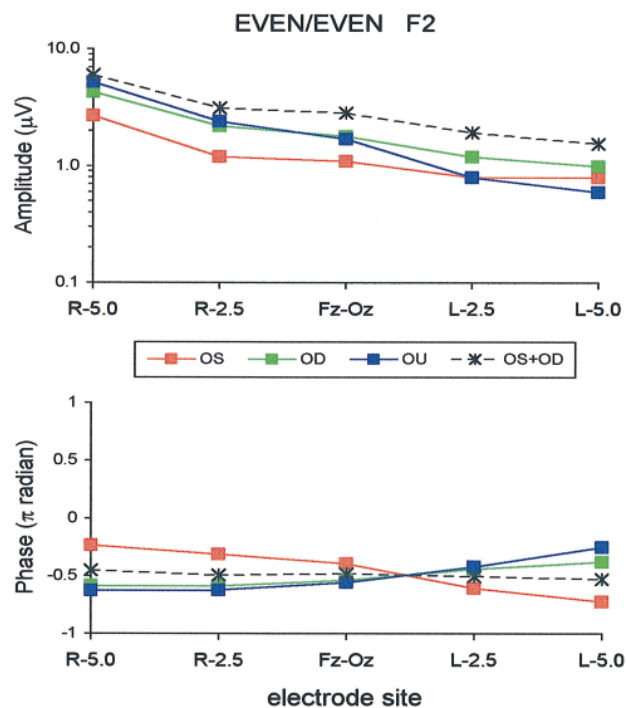
**Figure 8.** Fundamental (first harmonic) amplitude and phase of the responses to interchange between even and random isodipole textures. Responses are plotted as a function of scalp electrode placement at 2.5 cm. intervals from left and right of Oz. All leads were referenced to Fz.

**Figure 9.** Second harmonic responses to interchange between examples of even texture ensembles plotted as a function of scalp electrode placements of Figure 8.

comparisons of 2.0 and 2.8°/s gratings are ~60% correct, while velocity comparisons of 5.6 and 8.0°/s gratings are >80% correct.

Weber fractions for velocity discrimination calculated for low velocities (2.0–4.0°/s, Table 2) and high velocities (4.0–8.0°/s, Table 2) confirm these observations. For low velocities, impairment is remarkably large. Weber fractions are 3–4× normal for vertical drift. For horizontal drift, the lowest Weber fraction measured is 0.94 (OD). This is 6× normal, and indicates that velocity discrimination requires a 2-fold velocity difference. For OS and OU viewing of low-velocity horizontal drift, discrimination of even a 2-fold velocity difference is close to chance, so that a precise value of the Weber fraction cannot be reliably estimated (though one can be sure that it is >1, and thus at least 6× normal). In contrast, performance for high velocities (Table 2) is more nearly normal, with Weber fractions only 1.5× normal for vertical drift and 2.5× normal for horizontal drift.

*Comments*
Contrast sensitivity for horizontally oriented gratings was within the normal range, but contrast sensitivity for vertically oriented gratings was markedly reduced, consistent with the effects of greater retinal image blur for vertical targets because of ocular instability. Velocity discrimination was also much more impaired for vertical targets than for horizontal targets. Although the patient's fixation behavior was highly abnormal, the positional accuracy of the eyes was sufficient to perform the task, in that she had well-defined foveation periods with a target accuracy of at least ±30 min in both horizontal and vertical planes (Apkarian *et al.*, 1999). Near-chance psychophysical performance was

specific to horizontal drift, and occurred only for slow-velocity stimuli, which were randomly intermixed with the high-velocity stimuli. Neither acuity nor contrast sensitivity can account for these findings, since each stimulus was presented at a contrast set to 10× its measured detection threshold.

Although eye movements were not recorded during this task, the patient's oculomotor profile allows analysis of the extent to which performance may be accounted for by the intrinsic eye movement instabilities. The velocity range in which psychophysical performance fell to chance (<4°/s) corresponds closely to the minimum average eye velocities during foveation periods (Conte *et al.*, 1998, Apkarian *et al.*, 1999). In congenital nystagmus patients, non-fixational viewing also has been shown to contribute to judgements of flicker (Waugh and Bedell, 1992), based on the normal temporal contrast sensitivity functions. Such non-fixational viewing strategies may account for the worse performance for horizontal motion in this patient, since horizontal eye velocities were greater than vertical eye velocities during non-foveation periods, but not during foveation periods (Conte *et al.*, 1998; Apkarian *et al.*, 1999). Additionally, horizontal eye movement velocities across recording epochs are larger with binocular viewing than with either monocular viewing condition. These results may correspond to the psychophysical observation (Table 2) that, at low velocities, horizontal drift judgements are at chance with OU viewing, even though they are above chance with OD viewing.

***Kinetic Depth Effect***
In the kinetic depth effect (KDE) (Wallach and O'Connell, 1953),

the percept of a three-dimensional object is evoked by appropriately moving dots. In response to the KDE display, the patient reported a vivid shape percept (the normal response), and described the depicted three-dimensional shape accurately. The normal perception of a three-dimensional shape in the KDE indicates that the achiasmat's absence of stereopsis (see Clinical Profile) relates to the source of the three-dimensional information, rather than the ability to generate three-dimensional percepts *per se*. That is, brain mechanisms for extraction and representation of three-dimensional information appear to be relatively normal, even in the absence of binocular cues.

The velocities of the dots used in this study were in the range in which the patient's ability to discriminate velocities was impaired. This does not necessarily mean that velocity discrimination and implicit use of velocity differences are dissociated, since velocity difference thresholds for the KDE effect were not measured.

### Component and Plaid Motion

We sought to determine whether visual stimuli placed in corresponding areas of left and right hemifields interacted, and whether the patient would attend preferentially to visual input from the ipsilateral or contralateral hemifields when these inputs were in conflict. We reasoned that a superimposition of visual inputs from drifting gratings in corresponding points of the hemifields might lead to a combination of the gratings to form plaids (Adelson and Movshon, 1982), even if the anomalous superimposition were not in perfect spatial registry. As detailed in the Appendix, this study provided no evidence for anomalous interaction of inputs from the two halves of visual space.

### Visual Evoked Potentials

#### Motivation

Monocular full-field VEPs have been shown effective in demonstrating the misrouting of visual projections in albinos and achiasmats (Apkarian, 1991a,b; Apkarian *et al.*, 1995), but some visual stimuli (high-contrast transient pattern-onset checkerboards) demonstrate the misrouting more effectively than others. Checkerboard stimuli yield more robust VEP responses than comparably scaled stripes or grating patterns both in normal subjects, primarily due to the greater density of contours (Spekreijse *et al.*, 1973; Van Der Tweel, 1979), and in patients with oculomotor instabilities and/or optical aberrations such as astigmatism (Spekreijse, 1980; Apkarian, 1994). On a more neurophysiological level, the early portions of pattern-onset VEPs have a localized topography that typically is well described by one or two dipoles (Maier *et al.*, 1987; Van Dijk and Spekreijse, 1989), while stimuli such as flash and pattern-reversal VEP's generate responses from multiple areas and populations and require multiple dipoles to account for their scalp surface topography (Wood and Allison, 1981; Kraut *et al.*, 1985; Ducati *et al.*, 1988).

Thus, the observation that the VEP evidence of asymmetry is stimulus dependent reflects the multiple functional pathways by which visual information is transmitted to the brain and the fact that the contribution of these pathways depends on the visual image. To further investigate this dependence, we used VEP methods [isodipole texture interchange stimuli (Victor and Zemon, 1985; Victor, 1986) and windmill-dartboard stimuli (Zemon and Ratliff, 1982)] that separate responses related to processing of visual form from responses driven by luminance and/or contrast. These methods compare responses elicited by stimuli that are matched in spatial frequency content, and thus any resulting differences in the scalp topography must be due to neural processing, rather than optical or oculomotor factors.

#### Methods

Visual stimuli were presented on a background of 150 cd/m², and subtended an 8° square at the viewing distance of 57 cm. Isodipole textures (Victor and Zemon, 1985; Victor, 1986) were presented at a contrast of 0.4, a temporal frequency of 4.22 Hz and a check size of 16 min. Windmill-dartboard stimuli (Zemon and Ratliff, 1982) were presented at a contrast of 0.3. The VEP was recorded via standard gold cup electrodes placed on the scalp in a chain at 2.5 cm intervals across the occiput, from 5 cm to the left of Oz (Jasper, 1958) to 5 cm to the right of Oz, with recordings referred to a midline frontal lead placed at Fz. Signals were filtered (0.1–100 Hz), digitized at the frame rate of 270.3 Hz and averaged, with sweeps that contained artifacts (recognized as large voltage excursions) excluded. For each stimulus, three trials of 30 s were obtained. Fourier components were calculated from each of these trials, and confidence limits were obtained from the three trials via the $T_{circ}^2$ statistic (Victor and Mast, 1991). Each trial was run in three viewing conditions (OS, OD, OU).

#### Results and Comments

The fundamental (first harmonic) response elicited by isodipole interchange isolates intracortical processes related to extraction of visual form (Victor and Zemon, 1985; Victor, 1986). Its scalp topography, shown in Figure 8, demonstrated an ipsilateral projection pattern. OD viewing produced the largest response over the right occiput; OS viewing produced the largest response over the left occiput. Contralateral responses were small (<0.5 μV), thus precluding evaluation of interhemispheric phase shifts. These results suggest that this intracortically generated VEP response (Victor and Zemon, 1985; Victor, 1986; Victor and Conte, 1991), is driven by a purely ipsilateral geniculocalcarine projection.

The second-harmonic responses to interchange between members of identical isodipole texture ensembles is dominated by responses to local contrast, and does not require intracortical processing (Victor and Zemon, 1985; Victor, 1986). As shown in Figure 9, this response is largest over the right hemisphere for all viewing conditions, and does not demonstrate the ipsilateral-only projection pattern. Similar findings were obtained for the windmill-dartboard stimulus (data not shown), which generates responses due to local contrast interactions (Zemon and Ratliff, 1982). For this stimulus, responses were sufficiently robust across the electrode chain to examine interhemispheric differences in response timing via the phases of the Fourier components. As seen in Figure 9, OS responses occur earlier (i.e. have a phase shift that is less negative) over the right hemisphere than over the left hemisphere. OD responses occur earlier over the left hemisphere than over the right hemisphere. The phase *lead* of the contralateral response is ~0.4π radians (OS) and ~0.25π radians (OD). This corresponds to an effective latency reduction (at 2*f* = 8.45 Hz) of 24 ms (OS) and 15 ms (OD).

In summary, these findings indicate that the VEP correlates of intracortical pattern processing show an ipsilateral-only pattern (Fig. 8), while VEP signals that include contributions from contrast and luminance are distributed bilaterally (Fig. 9). The most direct interpretation of these findings is that, in addition to the ipsilateral-only geniculocalcarine projections that support pattern extraction (Fig. 8), there also are contralateral (or perhaps bilateral) projections that convey contrast and/or luminance information but do not contain sufficient detail (or are not used) to support the extraction of pattern. But it is also possible that the source structure is entirely ipsilateral in both cases, and

that contrast and luminance signals arise from a more complex pattern of dipole sources than pattern-processing signals and thus produce a bilateral scalp field (Shagass *et al.*, 1976; Barrett *et al.*, 1976; Skrandies and Lehmann, 1982; Maier *et al.*, 1987). Whatever the basis of their distinct topographies, the more widely distributed contrast and luminance responses have a shorter latency than the pattern-specific responses, both in normals (Victor and Zemon, 1985) and in this patient (Fig. 9). Thus, callosal transfer from an ipsilateral-only retinocortical projection pattern could not account for our results, since the second-harmonic responses (Fig. 9) over the contralateral hemisphere appear earlier than over the ipsilateral hemisphere.

Responses during binocular (OU) viewing were similar to responses elicited through OD alone, rather than what would be predicted by vector summation of OS and OD responses. This electrophysiological indication of suppression of OS signals was seen for the isodipole responses (Figs 8 and 9) as well as for the windmill-dartboard responses (not shown). Quantitative analysis of the non-additivity of monocular contributions (not shown) indicated that it was primarily present over the left hemisphere. In primary gaze, the patient has a horizontal misalignment of 20–25 prism diopters, and preferentially fixates with the right eye. If this misalignment is manifest under the viewing conditions for the VEP (8° field size at 57 cm), then the stimulus might well be viewed by the peripheral retina of the left eye, and thus have a reduced contribution to the VEP. However, suppression of left eye signals under binocular viewing conditions has also been observed in this patient with flash and flicker stimuli presented in a very wide field, in which lack of foveation cannot play a role (P. Apkarian, unpublished data).

## Visual Search

We examined performance on visual search (the ability to detect an 'oddball' rapidly amidst a field of visual distractors) under monocular viewing conditions. In subjects without a misrouting of visual pathways, the right hemisphere plays a dominant role in visual attention (Stone *et al.*, 1993; Gainotti, 1996), particularly for automatic attention and search tasks (Weintraub and Mesulam, 1988; Vilkki, 1989). If a corresponding asymmetry were also present in this subject, it could lead to poorer performance for stimulus presentation OD than OS. Additionally, any difference in salience of stimuli presented in the normal (contralateral) or anomalous (ipsilateral) representation might lead to differences in performance between visual fields, but not within each viewing condition. As detailed in the Appendix, we found no differences in performance with either eye, or in either hemifield.

## Visual Naming

In normal subjects who are left-hemisphere dominant for language, there is a difference in latency between verbal responses to visual information presented in the right and left hemifields (Saran and Davidson, 1989) attributed to the time required for interhemispheric transfer of information. If this patient, who is strongly right-handed, is left-brain dominant for language, then performance on visual naming tasks might be reduced in accuracy or prolonged in latency when stimuli are presented OD, as compared to OS. No differences in accuracy or latency were observed (see Appendix), although the resolution of the measurements might have been insufficient to identify the relatively subtle latency differences (~17–22 ms) that have been reported (Saran and Davidson, 1989).

## Auditory and Visual P300 (Oddball) Event-related Potentials

The 'oddball' P300, a parietocentral positivity occurring 300 ms after the presentation of task-specific stimulus, was described over 30 years ago and is clearly associated with attention, memory and cognitive processing of sensory information (Picton, 1992). Given the recognized hemispheric asymmetries in attentional mechanisms (Gainotti, 1996) and the alteration in sensory input, we wondered whether the achiasmatic state would be associated with a perturbation in this orienting attentional response. However, we found normal visual and auditory P300s, maximal in the central location despite lateralized presentation of information, indicating that the attentional systems as assessed by the P300 are not significantly altered in the achiasmatic state.

## Electroencephalography

### Motivation

It has been known since the earliest days of EEG recording (Berger, 1929) that the occipital alpha rhythm is blocked with eye opening, but it is unclear to what extent this is due to specific visual input, or rather, to general arousal. This patient's anomalous pattern of projections allows us to distinguish these possibilities, by determining whether alpha-blocking occurred only ipsilateral to an opened eye.

### Methods

The electroencephalogram was recorded via standard gold cup electrodes placed on the scalp in two parasagittal chains (anterior to posterior on the left: Fp1–F3, F3–C3, C3–P3, P3–O1; anterior to posterior on the right: Fp2–F4, F4–C4, C4–P4, P4–O2) according to the 10–20 system (Jasper, 1958). For each eye, two eye movement signals were derived from electrodes placed at three locations around each eye: outer canthus, upper margin; inner canthus, upper and lower margins. These signals (eight EEG, four EOG) were recorded on a Telefactor (West Conshohocken, PA) Beehive telemetry apparatus (sampling at 200 Hz, highpass filter at 0.3 Hz and lowpass filter at 70 Hz) along with a video image of the patient.

During most of the recording, the patient was asked to keep the eyes closed. During periods of quiet relaxation, the patient was asked to open the left eye, the right eye or both eyes for periods of several seconds. Segments of artifact-free EEG surrounding eye opening (12 or 13 trials each) were digitized. The instant of eye opening was determined by the onset of corresponding transients in the eye movement channels. From each segment, quantitative EEG analysis was performed on the 2 s interval preceding the eye-opening transient, and the 2 s period beginning 500 ms after the initial eye-opening transient. Power spectra and coherences were calculated by subdividing each 2 s period into three overlapping 1 s subintervals, followed by detrending, windowing and Fourier transformation of these subintervals. To eliminate possible contamination by eye-movement artifacts, only the two posterior channels on each side were analyzed (left: C3–P3, P3–O1; right: C4–P4, P4–O2). Paired *t*-tests based on log power were used to assess significance of any changes in spectral content or coherence.

### Results

Quantitative analysis of the EEG revealed a striking anomaly: the normal reduction in occipital alpha-band (from 8 to 12 Hz) activity associated with eye opening was seen predominantly in the hemisphere ipsilateral to the opened eye. As seen in the lower half of Figure 10, the occipital alpha-band power was reduced by 0.75 log units at P4–O2 following right eye opening, and 0.73 log unit power reduction at P3–O1 following left eye opening. Reduction in occipital alpha-band power contralateral to an open eye was more modest: 0.50 log units at P3–O1
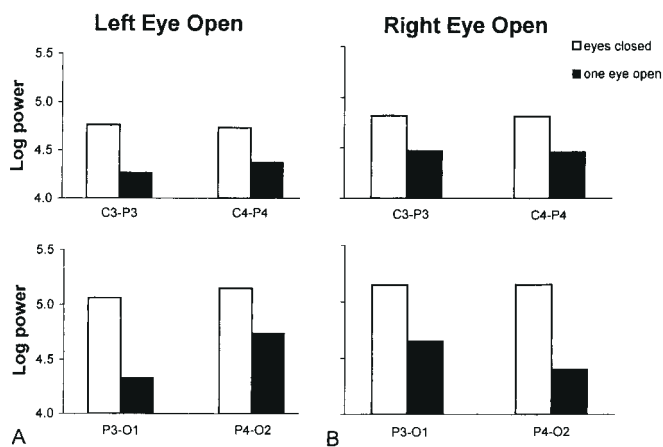
**Figure 10.** EEG spectral power at left (C3–P3, P3–O1) and right (C4–P4, P4–O2) posterior parasaggital channels, before (white) and after (black) left eye opening (*A*) and right eye opening (*B*). In each panel, data are organized in a semi-anatomical fashion (occipital leads in the lower half, parietal leads in the upper half; left- and right-sided channels on the corresponding sides of each panel. Power in the 8–12Hz band is estimated from multiple 2 s epochs immediately before and after unilateral eye opening to command.

following right eye opening, and 0.42 log units at P4–O2 following left eye opening. The differences between ipsilateral and contralateral reductions in occipital alpha-band power were statistically significant ($P = 0.036$ for left eye opening; $P = 0.053$ for right eye opening; $P = 0.007$ for the combined dataset).

As seen in the upper half of Figure 10, the predominantly unilateral reduction in alpha power was not seen in the more anterior channels (C3–P3 and C4–P4). The same pattern of ipsilateral > contralateral suppression of the alpha rhythm, confined to the occipital channels, was seen when the analysis was restricted to 9–11 Hz or 10 Hz alone.

Other aspects of the EEG were normal, including a normal organization of the background activity (low-voltage beta activity anteriorly and higher-voltage alpha activity posteriorly). Opening of both eyes led to reductions in alpha-band power comparable to what was observed with unilateral eye opening, without interhemispheric asymmetry.

We also calculated coherence between C3–P3 and C4–P4, and between P3–O1 and P4–O2, during eyes-closed and eyes-open states. Coherence in the alpha band was reduced from 0.45–0.54 to 0.27–0.51 with eye opening, suggestive of reduced interhemispheric correlations. However, these changes were of borderline statistical significance ($P = 0.05–0.25$, depending on the choice of spectral range), and without a clear anterior versus posterior pattern.

*Comments*

This analysis shows that the reduction in occipital alpha rhythm activity is predominantly ipsilateral to the open eye. It implies that the alpha generators in the two hemispheres are at least partially independent, and that occipital generators of alpha activity are blocked by visual input, rather than general arousal. More anteriorly, no ipsilateral versus contralateral difference was seen. This bilaterally symmetric reduction in alpha activity is consistent with changes in arousal, but is also consistent with the bilateral spread of visual activity via commissural pathways.

**Discussion**

This report describes some of the consequences of a rare developmental abnormality – isolated absence of the optic chiasm and consequent ipsilateral-only projection of the retinogeniculate pathways – for the anatomy and function of the visual system. Despite the gross miswiring of the retinogeniculocortical pathways, aspects of visual processing that depend on precise geometrical information, such as vernier acuity, texture perception and illusory contour formation, were normal, and there was no evidence for the confounding of visual information between the normal contralateral visual field representation and the anomalous ipsilateral visual field representation. Even three-dimensional object perception was intact, provided that the cue for depth did not require stereopsis, as shown by normal appreciation of the KDE.

The finding of normal vernier acuity thresholds is particularly striking, indicating that the remapping of retinal input has preserved the precise geometry of the topographic map necessary to support hyperacuity. On the other hand, there were disturbances in contrast sensitivity and velocity judgement, but their dependence on the orientation and velocity of the targets suggest that they were due to the ocular instabilities, rather than the miswiring *per se*. We did not find evidence that hemispheric specialization produced ocular asymmetries in performance, as might have been expected given the ipsilateral-only projection from each eye. While the lack of a demonstrable asymmetry might merely reflect an insufficient sensitivity of the measurements, interhemispheric communication (see below) most likely also plays a role.

Pathfinding at the chiasm is the subject of intense investigation, and appears due to interactions of retinotopically specific characteristics of retinal ganglion cell axons with local cues in the neighborhood of the developing optic chiasm (Baker and Reese, 1993; Sretavan and Reichardt, 1993; Guillery *et al.*, 1995; Marcus *et al.*, 1995; Sretavan *et al.*, 1995; Wang *et al.*, 1995; Chalupa *et al.*, 1996; Jeffery, 1997; Mason and Sretavan, 1997). Mechanisms that underlie postchiasmal pathfinding are less clear, but the implication of the current understanding of chiasmal pathfinding is that the postchiasmal course of fibers is determined by the retinal location of their origin, rather than the eye of origin or the region of visual space that they subserve. This is consistent with the findings of Williams *et al.* in achiasmatic dogs (Williams *et al.*, 1994); in these animals, fibers from the nasal and temporal hemiretinae of the same eye separate into layers at the lateral geniculate, as if they had originated from corresponding regions of the two eyes.

If, as Williams and co-workers suggest (Williams *et al.*, 1994), a common developmental rule for the geniculocortical projection applies in normals and achiasmats, then (i) a retinotopic map would be preserved within each hemifield, and (ii) projections from the mirror hemifields would be organized into alternating columns in the achiasmat, much as the projections from the two eyes are organized into alternating columns in normals. The fMRI studies presented here, in addition to confirming that each eye projects ipsilaterally to primary visual cortex (Fig. 1) as predicted from the initial VEP studies of this patient (Apkarian *et al.*, 1994a, 1995), supports this developmental rule for retinocortical projections. We find that stimulation of non-corresponding points in the two hemifields produces largely overlapping areas of activation within the ipsilateral hemisphere (Fig. 3), with preservation of at least a rudimentary topographic map (Fig. 4). Given the voxel size limitations of our images (1.6 mm), projections to neighboring columns would appear as largely overlapping, thus accounting for our observations. We speculate that, at a finer spatial

resolution, fibers from the nasal and temporal hemiretinae will be segregated into columns, even though they originate from the same eye and represent non-corresponding points of the visual field.

The visual abnormalities we have documented (i.e. the reduced acuity and the markedly elevated thresholds for velocity discrimination) do not appear to be related to the anomalous topographic map *per se* or its mirror-reversal nature, but rather to the oculomotor instabilities. The mechanisms of oculomotor instability in patients with congenital nystagmus and chiasmal misrouting, with or without albinism, are unclear. Postulated mechanisms include misrepresentation of stimulus velocity (Halmagyi *et al.*, 1980) or a combination of stimulus velocity and eye position (Optican and Zee, 1984).

It is interesting to compare this patient's performance on the vernier task with that of patients with horizontal congenital nystagmus. Although vernier thresholds are relatively insensitive to image drift in normals (Carney *et al.*, 1995), congenital nystagmus patients have higher thresholds for displacements along the horizontal axis (Bedell and Ukwade, 1997), ranging from 15 to 55 arc sec. These authors noted higher thresholds for horizontally than vertically separated targets. For the patient reported here, the comparable vernier threshold was at the lower end of this range, namely 15 arc sec.

In addition to the altered retinocortical map, there may be indirect developmental consequences of the chiasmal anomaly. Competition from fibers from the contralateral eye appears to be important in development (Taylor and Guillery, 1995). Neonatal section of the chiasm can reduce the number of visual transcallosal fibers (Boire *et al.*, 1995), and the pattern of retinal inputs may be important in shaping the distribution of visual callosal neurons (Chalupa *et al.*, 1996).

Despite the striking developmental anomaly, the achiasmat achieves behaviorally normal vision in most regards, without any evidence either of interference of stimuli in opposite hemifields or of disconnection. The lack of interference may reflect anatomical segregation at the columnar level (as discussed above). Even if the neuronal populations that subserve each hemifield are anatomically intermingled, functionally independent circuits may arise through Hebbian or other developmental rules. This is because the visual activity in adjacent areas within a single hemifield is highly correlated, while visual activity across mirror locations is largely uncorrelated.

To achieve relatively normal visual perception and visuomotor behavior with either eye, visual information must be transferred efficiently between the hemispheres. In the experimental animal, multiple pathways for interhemispheric transfer of visual information have been identified, including the corpus callosum (Maffei *et al.*, 1986; Ringo, 1993; Tardif *et al.*, 1997) and the anterior commissure (Ringo, 1993; Doty *et al.*, 1994), and brainstem pathways (Ringo and O'Neill, 1993; Doty *et al.*, 1994) — all of which are anatomically normal in this patient to the degree discernible by MRI.

Furthermore, animal studies suggest that interhemispheric transfer of information is relatively more important for extrastriate than for striate areas (Ringo, 1993; Tardif *et al.*, 1997). This is consistent with the EEG analysis (Fig. 10): unilateral eye opening suppresses the alpha rhythm over the occipital area primarily on the ipsilateral side, but more anteriorly, the suppression is equally present ipsilaterally and contralaterally. Physiological indications of interactions of signals from the two eyes is provided by the VEP studies (Fig. 9), in which the binocular responses deviate significantly from the arithmetic sum of the monocular responses. The fMRI studies indicate that interhemispheric transfer of information reflects not just anatomical connectivity, but is at least partially task-dependent. For passive viewing of a checkerboard, contralateral activation was extrastriate and seen only with viewing OD (Fig. 1). For passive viewing of illusory contour stimuli (Fig. 5), contralateral activation was seen with viewing OS or OD, but was again restricted to extrastriate cortex. For the picture naming task (Fig. 6), contralateral activation was also seen with viewing OS or OD, but was marked, and included both striate and extrastriate cortex. We postulate that the striate cortical inputs from the contralateral eye reflect feedback pathways from anterior 'higher-order' to 'lower-order' areas, whose existence is well recognized (Lund, 1988; Felleman and Van Essen, 1991; Bullier and Nowak, 1995) but whose functional role remains as yet undetermined.

Together, these results reveal a remarkable plasticity of retinal projections and human cortical organization. But we also found evidence that this plasticity is subject to certain limits. Although visual signals from the two eyes reach common areas of visual cortex, the patient has previously been shown to lack stereoscopic depth perception (see Clinical Profile). This suggests that the computations that support stereopsis require the presence of the direct geniculocortical afferents from corresponding retinal points, and not just interaction via feedback pathways or midline pathways, e.g. the corpus callosum. Right-hemisphere specialization for form analysis, as manifest by the right-hemisphere predominance of areas activated by illusory contours, had previously been observed in normal subjects (Hirsch *et al.*, 1995). This organization, which required interhemispheric transfer of low-level visual information, was present in this patient as well, rather than the alternative organization of bilateral areas sensitive to illusory contours.

Address correspondence to Jonathan D. Victor or Joy Hirsch, Department of Neurology and Neuroscience, Weill Medical College of Cornell University, 1300 York Avenue, New York, NY 10021, USA. Email: jdvicto@med.cornell.edu.

## References

Abadi RV, Dickinson CM (1986) Waveform characteristics in congenital nystagmus. Doc Ophthalmol 64:153–167.

Abadi RV, Pascal E (1991) Visual resolution limits in human albinism. Vis Res 31:1445–1447.

Abadi RV, Pascal E, Whittle J, Worfolk R (1989) Retinal fixation behaviour in human albinos. Optom Vis Sci 66:267–280.

Abel LA (1989) Ocular oscillations. Congenital and acquired. Bull Soc Belge Ophthalmol 237:163–189.

Adelson EH, Movshon JA (1982) Phenomenal coherence of moving visual patterns. Nature 300:523–525.

Apkarian P (1991a) Albinism. In: Principles and practice of clinical electrophysiology of vision (Heckenlively JR, Arden GB, eds), pp. 773–782. St Louis: Mosby Year Book.

Apkarian P (1991b) Methodology of testing for albinism with visual evoked cortical potentials. In: Principles and practice of clinical electrophysiology of vision (Heckenlively JR, Arden GB, eds), pp. 425–434. St Louis: Mosby Year Book.

Apkarian P (1994) Visual evoked potential assessment of visual function in pediatric neuroophthalmology. In: Principles and practice of ophthalmology (Albert DM, Jakobiec FA, eds), pp. 622–647. Philadelphia: W.B. Saunders.

Apkarian P (1996) Chiasmal crossing defects in disorders of binocular vision. Eye 10:222–232.

Apkarian P, Bour L, Barth PG (1994a) A unique achiasmatic anomaly detected in non-albinos with misrouted retinal–fugal projections. Eur J Neurosci 6:501–507.

Apkarian P, Dell'Osso LF, Ferraresi A, van der Steen J. (1994b) Ocular motor abnormalities in human achaismatic syndrome. Invest Ophthalmol Vis Sci 35(Suppl.):1410.

Apkarian P, Bour LJ, Barth PG, Wenniger-Prick L, Verbeeten B Jr. (1995) Non-decussating retinal–fugal fibre syndrome. An inborn achiasmatic malformation associated with visuotopic misrouting, visual evoked potential ipsilateral asymmetry and nystagmus. Brain 119:1195–1216.

Apkarian P, Bour L, Wenniger-Prick L, De Faber JTHN (1997) How does albino or achiasmatic misrouting of the visual pathways affect visual function and concomitant ocular motor control? Tijdschr Nederlandse Ver Orthop 2:39–49.

Apkarian P, Bour LJ, Van Der Steen J, Collewijn H (1999) Ocular motor disorders associated with inborn chiasmal crossing defects; multi-planar eye movement recordings in see-saw and congenital nystagmus. In: Current oculomotor research: physiological and psychological aspects (Becker W, Deubel H, Mergner T, eds), pp. 403–413. New York: Plenum Press.

Baker GE, Reese BE (1993) Chiasmatic course of temporal retinal axons in the developing ferret. J Comp Neurol 330:95–104.

Barrett G, Blumhardt L, Halliday AM, Halliday E, Kriss, A (1976) A paradox in the lateralisation of the visual evoked response. Nature 261:253–255.

Bedell HE, Ukwade MT (1997) Sensory deficits in congenital nystagmus. In: Basic and clinical aspects of vision science (Lakshminarayanan V, ed.), pp. 251–255. Dordrect: Kluwer.

Berger H (1929) Über das Elektroenzephalogramm des Menschen. Arch Psychiat Nervenkr 87:527–570.

Boire D, Morris R, Ptito M, Lepore F, Frost DO (1995) Effects of neonatal splitting of the optic chiasm on the development of feline visual callosal connections. Exp Brain Res 104:275–286.

Bullier J, Nowak LC (1995) Parallel versus serial processing: new vistas on the distributed organization of the visual system. Curr Opin Neurobiol 5:497–503.

Carney T, Silverstein DA, Klein SA (1995) Vernier acuity during image rotation and translation: visual performance limits. Vis Res 35:1951–1964.

Chalupa LM, Meissirel C, Lia B (1996) Specificity of retinal ganglion cell projections in the embryonic rhesus monkey. Perspect Dev Neurobiol 3:223–231.

Collewijn H, Apkarian P, Spekreijse H (1985) The oculomotor behaviour of human albinos. Brain 108:1–28.

Conte MM, Victor JD, Apkarian P (1998) Positional acuity and velocity discrimination in an achiasmat with see-saw and congenital nystagmus. Invest Ophthalmol Vis Sci 39(Suppl):400.

Cooper ML, Blasdel GG (1980) Regional variation in the representation of the visual field in the visual cortex of the Siamese cat. J Comp Neurol 193:237–253.

Creel DJ, Sheridan CL (1966) Monocular acquisition and interocular transfer in albino rats with unilateral striate ablations. Psychonom Sci 6:89–90.

Daroff RB, Troost BT, Dell'Osso LF (1978) Nystagmus and related ocular oscillations. In: Neurophthalmology (Glaser JS, ed.), pp. 219–240. Hagerstown: Harper & Row.

Doty RW, Ringo JL, Lewine JD (1994) Interhemispheric sharing of visual memory in macaques. Behav Brain Res 64:79–84.

Ducati A, Fava E, Motti EDF (1988) Neuronal generators of the visual evoked potentials: intracerebral recording in awake humans. Electroenceph Clin Neurophysiol 71:89–99.

Dutton JJ (1994) Gliomas of the anterior visual pathway. Surv Ophthalmol 38:427–452.

Elekessy EI, Campion JE, Henry GH (1973) Differences between the visual fields of Siamese and common cats. Vis Res 13:2533–2543.

Engel SA, Glover GH, Wandell BA (1997) Retintopic organization in human visual cortex and the spatial precision of functional MRI. Cereb Cortex 7:181–192.

Felleman DJ, Van Essen DC (1991) Distributed hierarchical processing in the primate cerebral cortex. Cereb Cortex 1:1–47.

Ferman LH, Collewijn H, Jansen TC, Van Den Berg AV (1987) Human gaze stability in horizontal, vertical and torsional direction during voluntary head movements, evaluated with a three-dimensional scleral induction coil technique. Vis Res 27:811–828.

Ffytche DH, Zeki S (1996) Brain activity related to the perception of illusory contours. NeuroImage 3:104–108.

Gainotti G (1996) Lateralization of brain mechanisms underlying automatic and controlled forms of spatial orienting of attention. Neurosci Biobehav Rev 20:617–622.

Gross KJ, Hickey TL (1980) Abnormal laminar patterns in the lateral geniculate nucleus of an albino monkey. Brain Res 190:231–237.

Guillery RW (1986) Neural abnormalities of albinos. Trends Neurosci 8:364–367.

Guillery RW (1990) Normal and abnormal visual field maps in albinos: central effects of non-matching maps. Ophthal Paediatr Genet 3:177–183.

Guillery RW (1996) Why do albinos and other hypopigmented mutants lack normal binocular vision, and what else is abnormal in their central visual pathways? Eye 10:217–221.

Guillery RW, Kaas JH (1971) A study of normal and congenitally abnormal retino-geniculate projections in cats. J Comp Neurol 143:73–100.

Guillery RW, Casagrande VA (1977) Studies of the modifiability of the visual pathways in Midwestern Siamese cats. J Comp Neurol 174:15–46.

Guillery RW, Hickey TL, Kaas JH, Felleman DJ, Debruyn EJ, Sparks DL (1984) Abnormal central visual pathways in the brain of an albino green monkey (Cercopithecus aethiops). J Comp Neurol 226:165–183.

Guillery RW, Mason CA, Taylor JSH (1995) Developmental determinants at the mammalian optic chiasm. J Neurosci 15:4727–4737.

Halmagyi GM, Gresty MA, Leech J (1980) Reversed optokinetic nystagmus (OKN): mechanism and clinical significance. Ann Neurol 7:429–435.

Hirsch J, DeLaPaz R, Relkin N, Victor J, Kim K, Li T, Borden P, Rubin N, Shapley R (1995) Illusory contours activate specific regions in human visual cortex: functional magnetic resonance imaging (fMRI) evidence for perceptual grouping processes. Proc Natl Acad Sci USA 92:6469–6473.

Hirsch J, Victor J, Kim K, Lee KM, Relkin R, Apkarian P (1997) fMRI mapping of visual projections in an achiasmatic subject. Invest Ophthalmol Vis Sci 38(Suppl):623.

Hubel DH, Wiesel TN (1971) Aberrant visual projections in the Siamese cat. J Physiol 218:33–62.

Jacobson SG, Mohindra I, Held R, Dryja TP, Albert DM (1984) Visual acuity development in tyrosinase negative oculocutaneous albinism. Doc Ophthalmol 56:337–344.

Jasper, HH (1958) The ten–twenty electrode system of the International Federation. Electroenceph Clin Neurophysiol 10:371–375.

Jeffery G (1997) The albino retina: an abnormality that provides insight into normal retinal development. Trends Neurosci 20(4):165–169.

Kaas JH, Guillery RW (1973) The transfer of abnormal visual field representations from the dorsal lateral geniculate nucleus to the visual cortex in Siamese cats. Brain Res 59:61–95.

Kaplan EF, Goodglass H, Weintraub S (1983) The Boston Naming Test, 2nd edn. Philadelphia: Lea & Febiger.

Kaufman LM, Miller MT, Mafee MF (1989) Magnetic resonance imaging of pituitary stalk hypoplasia. Arch Ophthalmol 107:1485–1489.

Kim KHS, Relkin NR, Lee KM, Hirsch J (1997) Distinct cortical areas associated with native and second languages. Nature 388:171–174.

Kraut MA, Arezzo JC, Vaughan HG Jr. (1985) Intracortical generators of the flash VEP in monkeys. Electroenceph Clin Neurophysiol 62:300–312.

Leigh RJ, Zee DS (eds) (1991) The neurology of eye movements, 2nd edn. Philadelphia: Davis.

Levi DM, Klein SA (1985) Vernier acuity, crowding, and amblyopia. Vis Res 25:979–991.

Loop MS, Frey TJ (1981) Critical flicker fusion in Siamese cats. Exp Brain Res 43:65–68.

Loshin DS, Browning RA (1983) Contrast sensitivity in albinotic patients. Am J Optom Physiol Opt 6:158–166.

Lund RD (1965) Uncrossed visual pathways of hood and albino rats. Science 149:1506–1507.

Lund JS (1988) Anatomical organization of macaque monkey striate visual cortex. Annu Rev Neurosci 11:253–288.

MacCarty CS, Boyd AS, Childs DS (1970) Tumors of the optic nerve and optic chiasm. J Neurosurg 33:439–444.

Maddox EE (1914) See-saw nystagmus with bitemporal hemianopsia. Proc R Soc Med 7:12–13.

Maffei L, Berardi N, Bisti S (1986) Interocular transfer of adaptation after effect in neurons of Area 17 and 18 of split chiasm cats. J Neurophysiol 55:966–976.

Maier J, Dagnelie G, Spekreijse H, Van Dijk B (1987) Principal components analysis for source localization of VEPs in man. Vis Res 27:165–177.

Maitland CG, Abiko S, Hoyt WF, Wilson CS, Okamura T (1982) Chiasmal apoplexy. J Neurosurg 56:118–122.

Marcus RC, Blazeski R, Godement P, Mason CA (1995) Retinal axon divergence in the optic chiasm: uncrossed axons diverge from crossed axons within a midline glial specialization. J Neurosci 15:3716–3729.

Mason CA, Sretavan DW (1997) Glia, neurons, and axon pathfinding during optic chiasm development. Curr Opin Neurobiol 7:647–653.

Mendola JD, Dale AM, Liu AK, Tootell RBH (1997) The representation of illusory contours in human visual cortex revealed by fMRI. Invest Ophthalmol Vis Sci 38(Suppl):204.

Menezes A, Lewis TL, Buncic JR (1996) Role of ocular involvement in the prediction of visual development and clinical prognosis in Aicardi syndrome. Br J Ophthalmol 80:805–811.

Milkman N, Schick G, Rossetto M, Ratliff F, Shapley R, Victor JD (1980) A two-dimensional computer-controlled visual stimulator. Behav Res Methods Instrum 12:283–292.

Oldfield RC (1971) The assessment and analysis of handedness. The Edinburgh inventory. Neuropsychologia 9:97–113.

Optican LM, Zee DS (1984) A hypothetical explanation of congenital nystagmus. Biol Cybernet 50:119–134.

Østerberg G (1938) Traumatic bitemporal hemianopsia (sagittal tearing of the optic chiasma). Acta Ophthalmol 16:466–474.

Pérez-Carpinell J, Capilla P, Illueca C, Morales J (1992) Vision defects in albinism. Optom Vis Sci 69:623–628.

Petry S, Meyer G (1987) The perception of illusory contours. New York: Springer-Verlag.

Picton TW (1992) The P300 wave of the human event-related potential. J Clin Neurophysiol 9:456–497.

Ringach D, Shapley R (1996) Spatial and temporal properties of illusory contours and amodal boundary completion. Vis Res 36:3037–3050.

Ringo JL (1993) The medial temporal lobe in encoding, retention, retrieval and interhemispheric transfer of visual memory in primates. Exp Brain Res 96:387–403.

Ringo JL, O'Neill SG (1993) Indirect inputs to ventral temporal cortex of monkey: the influence on unit activity of alerting auditory input, interhemispheric subcortical visual input, reward, and the behavioral response. J Neurophysiol 70:2215–2225.

Robinson DA (1963) A method of measuring eye movement using a scleral search coil in a magnetic field. IEEE Trans Biomed Electron 10:137–145.

Roessmann U (1989) Septo-optic dysplasia (SOD) or DeMorsier Syndrome. J Clin Neuro-ophthalmol 9:156–159.

Rubin N, Nakayama K, Shapley R (1995) Enhanced perception of illusory contours in the lower vs. the upper visual hemifields. Science 271:651–653.

Saran CD, Davidson RJ (1989) Reliability of visual evoked response estimates of interhemispheric transfer time: further studies. Psychophysiology 26:S53.

Schall JD, Ault SJ, Vitek DJ, Leventhal AG (1988) Experimental induction of an abnormal ipsilateral visual field representation in the geniculocortical pathway of normally pigmented cats. J Neurosci 8:2039–2048.

Shagass C, Amadeo M, Roemer RA (1976) Spatial distribution of potentials evoked by half-field pattern-reversal and pattern-onset stimuli. Electroenceph Clin Neurophysiol 41:609–622.

Shatz C (1977) A comparison of visual pathways in Boston and Midwestern Siamese cats. J Comp Neurol 171:205–228.

Skrandies W, Lehmann D (1982) Spatial principal components of multichannel maps evoked by lateral visual half-field stimuli. Electroenceph Clin Neurophysiol 54:662–667.

Snodgrass JG, Vanderwart M (1980) A standardized set of 260 pictures: norms for name agreement, familiarity, and visual complexity. J Exp Psychol Learn Mem Cognit 6:174–215.

Spekreijse H (1980) Pattern evoked potentials: principles, methodology and phenomenology. In: Evoked potentials (Barber C, ed.), pp. 55–74. London: MTP Press.

Spekreijse H, Van Der Tweel LH, Zuidema TH (1973) Contrast evoked responses in man. Vis Res 13:1577–1601.

Sretavan DW, Pure E, Siegel MW, Reichardt LF (1995) Disruption of retinal axon ingrowth by ablation of embryonic mouse chiasm neurons. Science 269:98–101.

Sretavan DW, Reichardt LF (1993) Time-lapse video analysis of retinal ganglion cell axon pathfinding at the mammalian optic chiasm: growth cone guidance using intrinsic chiasm cues. Neuron 10:761–777.

Stone J, Campion JE, Leicester J (1978) The naso-temporal division of the retinal in the Siamese cat. J Comp Neurol 180:783–798.

Stone SP, Halligan PW, Greenwood RJ (1993) The incidence of neglect phenomena and related disorders in patients with an acute right or left hemisphere stroke. Age Ageing 22:46–52.

Street RF (1931) A gestalt completion test. Contributions to education No. 481. New York: Bureau of Publications, Teachers College, Columbia University.

Talairach J, Tournoux P (1988) Co-planar stereotaxic atlas of the human brain. New York: Thieme-Verlag.

Tardif E, Richer L, Bergeron A, Lepore F, Guillemot J (1997) Spatial resolution and contrast sensitivity of single neurons in Area 19 of split-chiasm cats: a comparison with primary visual cortex. Eur J Neurosci 9:1929–1939.

Taub E, Victor JD, Conte MM (1997) Nonlinear preprocessing in short-range motion. Vis Res 37:1459–1477.

Taylor JSH, Guillery RW (1995) Effect of a very early monocular enucleation upon the development of the uncrossed retinofugal pathway in ferrets. J Comp Neurol 357:331–340.

Taylor WOG (1975) Albinism and colour defects. Mod Prob Ophthalmol 17:292–298.

Taylor WOG (1978) Visual disabilities of oculocutaneous albinism and their alleviation. Trans Ophthalmol Soc UK 98:423–445.

Traquair HM, Dott NM, Russell WR (1935) Traumatic lesions of the optic chiasma. Brain 58:398–411.

Treisman A (1982) Perceptual grouping and attention in visual search for features and for objects. J Exp Psychol Hum Percept Perform 8:194–214.

Truex RC, Carpenter MB (1969) Human neuroanatomy. Baltimore: Williams & Wilkins.

Van Der Tweel LH (1979) Pattern evoked potentials: facts and considerations. In: Proceedings of the XVIth Symposium of the International Society for Clinical Electrophysiology of Vision: Morioka, 24–28 May 1978, pp. 27–46. Tokyo: Japanese Journal of Ophthalmology.

Van Dijk BW, Spekreijse H (1989) Localization of the visually evoked response: The pattern appearance response. In: Topographic brain mapping of EEG and evoked potentials (Maurer K, ed.), pp. 360–365. Berlin: Springer-Verlag.

Victor JD (1986) Isolation of components due to intracortical processing in the visual evoked potential. Proc Natl Acad Sci USA 83:7984–7988.

Victor JD, Zemon V (1985) The human visual evoked potential: analysis of components due to elementary and complex aspects of form. Vis Res 25:1829–1844.

Victor JD, Conte MM (1991) Spatial organization of nonlinear interactions in form perception. Vis Res 31:1457–1488.

Victor JD, Mast J (1991) A new statistic for steady-state evoked potentials. Electroenceph Clin Neurophysiol 78:378–388.

Victor JD, Maiese K, Shapley R, Sidtis J, Gazzaniga MS (1989) Acquired central dyschromatopsia: analysis of a case with preservation of color discrimination. Clin Vision Sci 4:183–196.

Vilkki J (1989) Hemi-inattention in visual search for parallel lines after focal cerebral lesions. J Clin Exp Neuropsychol 11:319–331.

Wallach H, O'Connell DN (1953) The kinetic depth effect. J Exp Psychol 45:205–217.

Walsh FB (1956) The ocular signs of tumors involving the anterior visual pathways. Am J Ophthalmol 42:347–377.

Wang L, Dani J, Godement P, Marcus RC, Mason CA (1995) Crossed and uncrossed retinal axons respond differently to cells of the optic chiasm midline *in vitro*. Neuron 15:1349–1364.

Wasserstein J, Zappulla R, Rosen J, Gerstman L, Rock D (1987) In search of closure: subjective contour illusions, Gestalt completion tests, and implications. Brain Cogn 6:1–14.

Waugh SJ, Bedell HE (1992) Sensitivity to temporal luminance modulation in congenital nystagmus. Invest Ophthalmol Vis Sci 33:2316–2324.

Weintraub S, Mesulam MM (1988) Visual hemispatial inattention: stimulus parameters and exploratory strategies. J Neurol Neurosurg Psychiat 51:1481–1488.

Williams RW, Dell'Osso LF (1993) Ocular motor abnormalities in achiasmatic mutant Belgian sheepdogs. Invest Ophth Vis Sci 34, 1135.

Williams RW, Hogan D, Garraghty PE (1994) Target recognition and visual maps in the thalamus of achiasmatic dogs. Nature 367:637–639.

Wilson HR, Mets MB, Nagy SE, Kressel AB (1988) Albino spatial vision as an instance of arrested visual development. Vis Res 28:979–990.

Wolfe J (1994) Guided Search 2.0: a revised model of visual search. Psychonom Bull Rev 1:202–238.

Wood CC, Allison T (1981) Interpretation of evoked potentials: a neurophysiological perspective. Can J Psychol 35:113–135.

Woods RP, Mazziotta JC, Cherry SR (1993) MRI–PET registration with automated algorithm. J Comput Assist Tomogr 17:536–546.

Yee RD, Wong EK, Baloh RW, Honrubia V (1976) A study of congenital nystagmus waveforms. Neurology 26:326–333.

Zemon V, Ratliff F (1982) Visual evoked potentials: evidence for lateral interactions. Proc Natl Acad Sci USA 79:5723–5726.

## Appendix

### Illusory contour formation

Kanizsa square stimuli (see Fig. 5) were presented on the monitor of an SGI Indigo 2 computer at a retinal eccentricity of 10° from the fixation point on a background luminance of 50 cd/m$^2$, at a contrast of 0.3. Spatial parameters were similar to those used in studying normal subjects (Rubin *et al.*, 1995; Ringach and Shapley, 1996). In particular, the support ratio of the Kanizsa square (the ratio of the diameter of a single inducer to the distance between the centers of the inducing elements) was 0.4. Stimuli were presented for 0.5 s, and followed by a 0.7 s mask, to ensure that there was time for adequate foveation of the center of the display. This was subsequently reduced to 0.25 s, followed by a 0.7 s mask. (In normal control subjects, a presentation time of 0.05 s was used.) The patient viewed the stimuli monocularly. Each eye was tested separately in counterbalanced blocks following a familiarization trial with very slow stimuli.

We attempted to quantify the subjective strength of the illusory contours formed by the Kanizsa square via a strategy previously used in studying illusory contour perception in normal subjects (Rubin *et al.*, 1995; Ringach and Shapley, 1996). This strategy relies on the improvement in performance on a shape discrimination task when illusory contours are present (Rubin *et al.*, 1995). The patient was asked to discriminate between two slight distortions of a Kanizsa square, labeled 'thin' and 'fat', corresponding to the concave and convex curvatures of the vertical illusory contours induced by rotations of the inducers. In a control condition, the patient was asked to judge (again in a two-alternative, forced-choice task) local orientation of inducing elements all facing in the same direction, to preclude the presence of illusory contours (Ringach and Shapley, 1996). There were 32 presentations (two-alternative, forced-choice) per stimulus block, and altogether eight blocks of illusory contour stimuli and eight blocks of control stimuli. Thresholds (82% correct) for shape discrimination (from the illusory contour stimuli) and local orientation discrimination (from the control stimuli) were extracted by fitting the psychophysical performance to a sigmoid function.

The patient readily described the illusory contours with either eye. However, attempts to quantify the illusory contour strength via shape discrimination were unsuccessful, because even at the shorter stimulus duration (0.25 s) used, orientation thresholds were at ceiling for both the control task and when illusory contours were present: 0.83° (OD) and 0.93° (OS) under control conditions, and 0.83° (OD) and 0.83° (OS) with illusory contours present. All of these thresholds were lower than those obtained in normal subjects (who viewed much briefer presentations of the stimuli).

### Street Test

The Street test figures (Street, 1931), 17 in total, were presented monocularly, for presentation times of 1–2 s. The patient was tested first with only the right eye, then, following a break, with only the left eye. The patient was asked to identify each figure as rapidly as possible. Performance was rapid and perfect with either eye.

### Kinetic Depth Effect

The KDE (Wallach and O'Connell, 1953) was elicited by a computer (SGI Indigo 2) display which consisted of moving dots, whose flow was consistent with a transparent revolving sphere. The patient viewed the KDE sphere monocularly, first OD and then OS. Dots had a mean velocity of 4°/s and were presented for 30 s, the duration of the display.

### Component and Plaid Motion

Visual stimuli consisted of circular patches of drifting sinusoidal luminance gratings presented on an equiluminant field (8° square, mean luminance 150 cd/m$^2$, viewed at 57 cm). The gratings had a contrast of 0.5, a spatial frequency of 2 c/°, and a temporal frequency of 4 Hz, corresponding to a drift velocity of 2°/s. The circular apertures through which these gratings were visible were 3° in diameter and positioned with centers 4° apart (one in each quadrant of the display), equally spaced about a central fixation point. Stimuli were presented for 1 s, paced by the patient, in two blocks of 16 trials for each monocular (OS, OD) viewing condition. The patient was asked to indicate the direction of dominant motion by hand gesture to an experimenter who was positioned to observe the patient but not the display. The direction of motion was recorded when the experimenter was satisfied that the patient's intended response was understood. This approach was used to eliminate any possible left–right or language ambiguities. The patient was told to guess if necessary, and that there was not necessarily a 'correct' answer, and that valid answers included the four cardinal directions and the four diagonal directions.

In experiment A, four grating patches (one in each quadrant) were used. In each of these four-patch stimuli, two gratings (in diagonally related patches) drifted horizontally; the two gratings placed in the remaining patches drifted vertically. Either the horizontal or vertical pair was assigned to be drifting in the same direction, while the other pair of gratings drifted in opposing directions. Thus, each stimulus contained two gratings moving in one direction (e.g. upwards), and two gratings moving in opposing directions (e.g. one leftward and one rightward).

In experiment B, the stimuli of experiment A were modified by omitting two of the patches moving in the same direction. The remaining diagonally disposed patches contained either horizontal or vertical gratings, drifting in opposite directions, one in each hemifield. In both experiments, stimuli were balanced for all combinations of field, orientation and direction.

The stimuli of experiment A were designed such that if, under monocular viewing conditions, the patient perceived a superposition of the patches in one hemifield and a mirror-inversion of the patches in the contralateral hemifield (i.e. a mixture of inputs from corresponding points in an overlaid cortical representation), then patches of the stimuli would appear to be plaids drifting in a diagonal direction. However, a dominant diagonal direction of motion was never reported for any of the 64 trials, thus providing no evidence of abnormal interactions between overlaid representations.

The stimuli of experiment B were designed to determine whether, under monocular viewing conditions, the patient based judgments primarily on the ipsilateral or contralateral stimulus. All responses corresponded to the direction of one of the two opposing gratings, but there was no statistically significant bias in favor of the contralateral (normal) or ipsilateral (anomalous) representation.

### Visual Search

Parallel search (Treisman, 1982) was assessed by asking the patient to identify a visual target stimulus from an array of distractors. We used

test cards, as described elsewhere (Victor *et al.*, 1989), consisting of rectangles of various colors and orientations which subtended approximately 0.5° × 1° at the viewing distance of 30 cm. The patient was required to point at the single oddball stimulus among the 39 distractors in an 8 × 5 array. In the 'color' condition, the target rectangle had a color which was complementary to that of the distractors; orientations were randomly horizontal or vertical; brightness was also randomized. In the 'orientation' condition, the target had an orientation which was orthogonal to that of the distractors; color and brightness were also randomized. We also examined performance on a more difficult search task, the 'color × orientation' condition. In this condition, half of the distractors were of one color and one orientation (e.g. red and vertical), and the other half of the distractors were of the complementary color and orientation (e.g. green and horizontal); the target was an exception to this color–orientation pairing (e.g. red and horizontal). Each stimulus condition (color, orientation and color × orientation) was tested with two blocks of six cards, in each of three (OS, OD and OU) viewing conditions. Half of the targets were positioned in the left hemifield; half were in the right hemifield. Presentation order was counterbalanced to avoid practice effects.

For cards in which the oddball was distinguished by a single parameter (e.g. color or orientation), the patient was able to point to the oddball immediately, independent of hemifield of the target or viewing condition. These responses also were too rapid for manual stopwatch timing. For cards in which the identification of the oddball required joint processing of color and orientation, processing required 1 s/card (OD, OU) or 1.6 s/card (OS) (not significant), with no significant dependence on the visual hemifield that contained the target. Responses were within the normal range [mean, 1.2 s/card (Victor *et al.*, 1989)]. In debriefing, the patient indicated that in the single-modality conditions, the search task was easy and immediate. In the color × orientation task, the patient reported to have attended initially to one color and then to have looked for the oddball. If the oddball was not present, the patient then attended to targets of the other color − i.e. she used a strategy of a guided parallel search (Wolfe, 1994). Thus, search speed and accuracy were normal for targets projected to the left or right hemisphere. Within each hemisphere, there were no differences in performance for targets that were presented in the normal (contralateral) vs. the anomalous (ipsilateral) representation.

### Visual Naming
We employed a timed picture naming test (Neuroscan Inc., Herndon, VA). The color pictures were derived from the Snodgrass picture set (Snodgrass and Vanderwart, 1980) and were scaled to an average diameter of 3.3 × 7 cm. Each stimulus was presented for 1 s with an interstimulus interval of 3 ± 0.3 s. The patient's verbal responses in Dutch were recorded by the program from 200 to 2000 ms after the presentation. Response latency was calculated from the initial inflection of the digitalized audio sound. Response accuracy was rated by a translator fluent in Dutch. Pictures were presented as interleaved blocks of 9 or 10. Two blocks, with a total of 20 stimuli, were presented OU and three blocks, with a total of 29 stimuli, were presented both OS and OD.

The second block presented OD was identical to the third block presented OS; the third block OD was identical to the second block OS. The patient's responses were compared to that of three sex-matched controls aged 14, 16 and 27 years.

The patient's response accuracy (86%) did not differ significantly from that of the control subjects (86, 92, 97%). There was no significant difference ($P > 0.1$) between the patient's response latency and the average latency of the three control subjects (patient mean ± SD versus control mean ± SD): OU 945 ± 315 versus 910 ± 280 ms; OD 975 ± 438 versus 933 ± 225 ms; OS 928 ± 340 versus 945 ± 289 ms). There was no significant difference in the patient's verbal response time under the different viewing conditions ($P$ 0.1 for OD versus OU, OD versus OU, OS versus OU). There was no significant difference in mean response latency between blocks of identical stimuli presented first to OS and then to OD, or first to OD and then to OS ($P > 0.1$).

### Auditory and Visual P300 (Oddball) Event-related Potentials
Auditory and visual P300 (oddball) event-related potentials were measured to assess the integrity of the orienting response and sustained attention. EEG data were recorded from gold cup electrodes placed in sagittal and parasagittal chains (linked mastoid references) with a NeuroScan system. The EEG (DC to 100 Hz, digitally filtered) was recorded continuously and analyzed in 1024 ms epochs beginning 100 ms prior to the stimulus presentation. Vertical and horizontal eye movements were detected by EOG electrodes and epochs containing artifacts were rejected by an automatic algorithm.

For the visual task, the stimuli consisted of centered, high-contrast (white on black) shapes ('O' = frequent stimulus and 'X' = infrequent stimulus) subtending 8°, presented for 300 ms, with 3 + 0.3 s inter-stimulus intervals. For the auditory task, 85 dB tones of either 500 Hz (frequent tone) or 1000 Hz (infrequent tone) were presented via head-phones. The tone's duration was 0.5 s with an interstimulus interval of 2.5 + 0.3 s. For both stimulus types, EEG recordings from 200 presentations were collected over 11 min, with the infrequent stimulus presented in random order ~20% of the time. The task consisted of silent counting of the number of oddball stimuli in a trial, with a verbal report of the total at the end of each trial. For the visual task, EEG recordings were available for the OS and OU conditions only. For the auditory task, recordings were available for the AS (left ear), AD (right ear) and AU (binaural) conditions.

Each epoch was baseline corrected (from the recording during the 100 ms prior to the stimulus onset) and screened for eye movement artifact prior to averaging. The P300 was determined by subtraction of the averaged response to the frequent stimulus from the averaged response to the infrequent stimulus.

In all conditions, the P300 was maximal at Pz, and this response waveform was used to measure latency and amplitude. In the visual paradigm, the patient's P300 latency and amplitude were 394 ms and 22 µV (OU) and 392 ms and 24 µV (OS) respectively. There was no apparent difference between conditions. In the auditory paradigm, the patient's P300 latency and amplitude were 362 ms and 25 µV (AU), 360 ms and 17 µV (AD), and 404 ms and 23 µV (AS).